



**UNIVERSITÀ degli STUDI di ROMA
“TOR VERGATA”**

**DOTTORATO di RICERCA in
"BIOCHIMICA E BIOLOGIA MOLECOLARE"
2006/2009-XXII CICLO**

TESI

***BIOTIN-ANANDAMIDE: A NEW TOOL
TO VISUALIZE ANANDAMIDE INSIDE
THE CELLS***

Dott.ssa Chiara De Simone

Docente Guida *prof. Alessandro Finazzi-Agrò*

Correlatore *prof. Mauro Maccarrone*

Esaminatori *proff. P Sarti, R Knight, V De Laurenzi*

Coordinatore *prof. Alessandro Finazzi-Agrò*

DIPARTIMENTO DI MEDICINA SPERIMENTALE E SCIENZE BIOCHIMICHE
VIA MONTPELLIER, 1, 00133 ROMA

RIASSUNTO	5
ABSTRACT.....	6
INTRODUCTION.....	7
CHAPTER 1. THE ENDOCANNABINOID SYSTEM.....	12
1.1 Molecular targets.....	12
1.2 AEA metabolism.....	17
1.2.1 AEA biosynthesis.....	17
1.2.2 AEA degradation and uptake.....	18
1.3 2-AG metabolism.....	23
1.3.1 2-AG biosynthesis.....	23
1.3.2 2-AG degradation and uptake.....	24
CHAPTER 2. FLUORESCENT LIPID PROBES.....	27
CHAPTER 3. OBJECTIVES OF THE RESEARCH.....	30
CHAPTER 4. RESULTS.....	31
4.1 Characterization of b-AEA.....	31
4.2 Metabolism of AEA and b-AEA in HaCaT cells.....	33
4.3 Inhibition assays of AEA and b-AEA.....	35
4.4 Immunofluorescence studies of b-AEA accumulation.....	37
4.5 Visualization of b-AEA accumulation in lipid droplets.....	39

4.6 [3H]AEA accumulation in lipid droplets.....	40
4.7 Morpho-functional overlap between LDs and FAAH.....	41
4.8 Storage of [3H]AEA in adiposome-rich fractions of HaCaT cells.....	43
4.9 Identification of AEA-binding activity within the cytosol.....	45
4.10 Gel filtration and [3H]AEA-binding activity.....	46
4.11 Nano-LC ESI-MS/MS identification of affinity-purified AEA binding proteins.....	48
4.12 In vitro analysis of Hsp70-AEA interaction.....	50
4.13 Effect of Hsp70 overexpression on AEA uptake in SH-SY5Y cells...	51

CHAPTER 5. DISCUSSION.....53

CHAPTER 6. EXPERIMENTAL PROCEDURES.....58

6.1 Materials.....	58
6.2 Cell culture and treatments.....	59
6.3 Biochemical analyses.....	59
6.3.1 FAAH assay.....	59
6.3.2 NAPE-PLD assay.....	59
6.3.3 AMT assay.....	60
6.3.4 DAGl assay.....	60
6.3.5 MAGl assay.....	60
6.3.6 Receptor binding assay.....	61
6.4 Synthesis of b-AEA.....	61
6.5 Western blot analyses.....	61
6.6 Subcellular fractionation of [3H]AEA-treated cells.....	62
6.7 Extraction of cytosolic proteins.....	63

6.8 Fractionation by gel filtration.....	63
6.9 Biotin-affinity chromatography.....	64
6.10 Nano-LC ESI-MS/MS.....	64
6.11 [3H]AEA-binding assay by DEAE.....	64
6.12 Fluorescence microscopy studies.....	65
6.13 Statistical analysis.....	65
REFERENCES.....	66
SHORT CURRICULUM VITAE.....	85
LIST OF PUBLICATIONS.....	86
COPY OF RELAVANT PUBLICATIONS.....	87

RIASSUNTO

L'endocannabinoide anandamide è un lipide neuromodulatorio non carico che è inattivato grazie al suo assorbimento cellulare e successivo catabolismo. Mentre la biosintesi e la degradazione dell'anandamide sono state chiarite in dettaglio, il meccanismo attraverso cui essa entra all'interno della cellula rimane ancora non chiaro. Vi è un generale accordo solo sul fatto che il movimento dell'anandamide attraverso la membrana plasmatica è rapido, ha una cinetica di saturazione ed è temperatura dipendente. Mentre molti sono gli studi che descrivono un assorbimento mediato da uno specifico trasportatore di questo endocannabinoide, solo pochi lavori hanno proposto che il trasporto avvenga attraverso semplice diffusione passiva o attraverso endocitosi mediata da caveolae/lipid rafts. L'unica cosa certa però ad oggi è che, la mancanza del clonaggio e dell'espressione di questa ipotetica proteina trasportatrice, ha impedito lo sviluppo di strumenti molecolari che potrebbero dare una definitiva risposta della reale presenza di un trasportatore sulla superficie cellulare. Allo stesso tempo, non sono ancora stati messi a punto analoghi dell'anandamide che ci consentano di visualizzare i suoi movimenti attraverso la membrana plasmatica e di conseguenza il suo destino all'interno della cellula.

Il nostro gruppo ha sintetizzato e caratterizzato un analogo dell'anandamide (b-AEA) che possiede la stessa lipofilia del composto madre. Abbiamo usato metodi biochimici e di microscopia impiegando la b-AEA come strumento per visualizzare l'accumulo, la distribuzione ed i movimenti intracellulari dell'anandamide.

Abbiamo scelto di modificare la testa polare della molecola poiché questo cambiamento strutturale non influenza la cinetica del trasporto. I nostri studi ci hanno consentito di chiarire la presenza di strutture intracellulari dette adiposomi, che possono accumulare anandamide e che potrebbero essere coinvolti nel suo trasporto verso la FAAH. Usando la nostra molecola biotinilata abbiamo inoltre identificato due proteine citosoliche, l'albumina e la Hsp70.2, come potenziali trasportatori che legano l'anandamide e che potrebbero formare un sistema di trasporto in grado di consentire, in modo veloce ed efficiente, il movimento dell'anandamide all'interno della cellula.

ABSTRACT

ABSTRACT

The endocannabinoid anandamide is an uncharged neuromodulatory lipid that is inactivated through its cellular uptake and subsequent catabolism. While the biosynthesis and degradation of AEA have been clarified in considerable detail, the mechanism of AEA uptake has remained elusive. There is a general consensus only on the fact that AEA movement through the plasma membrane is rapid, saturable, temperature-dependent. While many studies describe a transporter-mediated uptake of AEA via a selective “anandamide membrane transporter”, only a few papers proposed that the transport occurs by simple diffusion or endocytosis via caveolae/lipid rafts. As a matter of fact, the lack of cloning and expression of the purported transporter protein has prevented the development of molecular tools which could give definitive proof of the presence of a true transporter on the cell surface. In the same line, AEA analogs able to visualize AEA movement across the plasma membrane and its subsequent fate within the cell, are still missing.

We synthesized and characterized a biotinylated analog of AEA (biotin-AEA) that has the same lipophilicity of the parent compound. We used biochemical assays and fluorescence microscopy employing b-AEA as a tool to visualize accumulation, intracellular distribution and trafficking of AEA inside the cells. We chose to modify the polar head of AEA because this structural change does not influence the kinetics of AEA uptake. Our studies led us to clarify the presence of molecular structures, the adiposomes, as a way to accumulate AEA and that could be involved in its delivery to FAAH. Using our biotinylated probe, we also identified two cytosolic proteins (albumin and Hsp70.2) as potential AEA-binding carriers which might form a delivery system to rapidly and efficiently assist the intracellular trafficking of AEA.

INTRODUCTION

In the last decades a growing interest was focused on the study of a particular family of endogenous lipids named endocannabinoids, raising the fate of an otherwise mistreated class of biomolecules.

The discovery of the major psychotropic component of the preparations from *Cannabis sativa*, the lipophilic compound Δ^9 - tetrahydrocannabinol (THC) (Gaoni and Mechoulam, 1964), was not immediately followed by the molecular characterization of the corresponding receptor in the mammalian brain (Di Marzo, 2009). The stringent structural characteristics that cannabinoid compounds must possess in order to exert their psychotropic effects and the important observation that cannabinoids inhibit adenylate cyclase (Howlett and Fleming, 1984) was the strong evidence for the presence of a specific, high-affinity binding site for those lipids. More than two decades had to be waited until the first THC-specific receptor, named cannabinoid receptor type-1 (CB1), could be first identified (Devane et al., 1988) and then cloned after the screening of several previously characterized orphan G-protein-coupled receptors (GPCRs) for their affinity for THC (Matsuda et al., 1990). The second cannabinoid receptor, named CB2, identified by means of homology cloning, turned out to be rather different from CB1 both in its amino acid sequence and its localization in mammalian tissues (Munro et al., 1993). Whilst CB1 was shown to be extremely abundant in the brain, and hence suggested to be responsible for THC psychoactivity, CB2 was expressed in its highest levels in immune cells. The cloning of the cannabinoid receptors opened the way to the identification of their endogenous ligands (Fig. 1). The first endocannabinoid to be discovered was anandamide (AEA, N-arachidonoyl-ethanolamine) (Devane et al., 1992), a finding soon to be followed by the observation that an already known endogenous metabolite, 2-arachidonoyl-glycerol (2-AG), also exhibits high affinity for CB1 and CB2 receptors (Mechoulam et al., 1995; Sugiura et al., 1995). Other endocannabinoids (Fig. 2) have also been proposed during the last 10 years, including 2-arachidonoyl-glycerol ether (noladin ether) (Hanus et al., 2001), N-arachidonoyl-dopamine (NADA) (Bisogno et al., 2000; Huang et al., 2002) and virodhamine (Porter et al., 2002), but their pharmacological activity

and metabolism has not yet been thoroughly investigated. Therefore, anandamide and 2-AG are still referred to as the “major” endocannabinoids. The catabolic pathways and enzymes for anandamide and 2-AG have been largely investigated and partly identified. N-Arachidonoyl-phosphatidylethanolamine (NArPE) and diacylglycerols (DAGs) with arachidonic acid on the 2-position act as the major biosynthetic precursors of anandamide (Di Marzo et al., 1994) and 2-AG (Di Marzo et al., 1996a; Bisogno et al., 1997; Stella et al., 1997), respectively. NArPE is produced from the transfer of arachidonic acid from the sn-1 position of phospholipids to the nitrogen atom of phosphatidylethanolamine (Cadas et al., 1997), whereas DAG precursors for 2-AG derive mostly from the phospholipase C-catalysed hydrolysis of phosphatidylinositol (Stella et al., 1997) and, in certain cells, from the hydrolysis of phosphatidic acid (Bisogno et al., 1999). The two endocannabinoids are inactivated essentially by enzymatic hydrolysis of their amide and ester bonds, and the major enzymes responsible for these reactions have been cloned from several mammalian species and are known as fatty acid amide hydrolase (FAAH) (Cravatt et al., 1996) and monoacylglycerol lipase (MAGL) (Karlsson et al., 1997; Dinh et al., 2002), for anandamide and 2-AG, respectively. Biosynthetic enzymes for endocannabinoids have been also cloned. Two sn-1-selective DAG lipases, named DAGL- α and DAGL- β , are responsible for 2-AG biosynthesis in cells and tissues (Bisogno et al., 2003), whereas the enzyme catalysing the direct conversion of NArPE into anandamide is known as N-acylphosphatidyl-ethanolaminespecific phospholipaseD (NAPE-PLD) (Okamoto et al., 2004). Finally, a specific process through which endocannabinoids, according to the direction of their gradient of concentrations across the plasma membrane, are either taken up by cells following cannabinoid receptor activation, or released from cells following endocannabinoid biosynthesis, has been proposed by some authors (Di Marzo et al., 1994; Beltramo et al., 1997; Beltramo and Piomelli, 2000; Bisogno et al., 2001), but not others (Glaser et al., 2003; Bracey et al., 2002). This mechanism appears to be pharmacologically distinct from FAAH or MAGL (Maione et al., 2008; Fowler and Ghafouri, 2008) or CB1 receptors (Ortega-Gutiérrez et al., 2004), although it not yet been identified from a molecular point of view. Several alternative enzymes for the biosynthesis of anandamide from NArPE, and for the inactivation of 2-AG to glycerol and arachidonic acid, have been recently proposed. Since NAPE-PLD “knock-out” mice do not exhibit reduced levels of anandamide in most tissues (Leung et al., 2006) this endocannabinoid was suggested to

be formed also from the sequential cleavage of the two sn-1 and 2- acyl groups of NArPE, catalysed by α/β -hydrolase 4, followed by the phosphodiesterase-mediated hydrolysis of glycerophosphoanandamide (Simon and Cravatt, 2006). The formation of phospho-anandamide from the hydrolysis of NArPE catalysed by phospholipase C enzyme(s), followed by its conversion into anandamide, is another possible biosynthetic route (Liu et al., 2006; Liu et al., 2008). Finally, the biosynthesis of anandamide might also occur via conversion of NArPE into 2-lyso-NArPE by a soluble form of phospholipase A2, followed by the action of a lysophospholipase D (Sun et al., 2004).

Moreover anandamide, but not 2-AG, has been found to be a ligand for transient receptor potential channel vanilloid type-1 (TRPV1) (De Petrocellis et al., 2001), supporting the involvement of cannabinoid and vanilloid receptors-independent pathways in various biological actions of endocannabinoids. The cannabinoid receptors, endocannabinoids and the proteins for their synthesis and inactivation constitute the “Endocannabinoid System” (ES).

Whilst the biosynthesis and degradation of AEA have been clarified in considerable detail, leading to the molecular cloning and characterization of the AEA hydrolase FAAH (McKinney and Cravatt, 2004) and of the AEA synthetase NAPE-PLD (Okamoto et al., 2004), the mechanism of AEA uptake has remained elusive, and to date a general consensus has been reached only on the fact that AEA movement through the plasma membrane is rapid, saturable, temperature-dependent, and energy (supplied as ATP or ion gradients)-independent (Battista et al., 2005; Glaser et al., 2005; Hillard and Jarrahian, 2005). Against >100 papers describing a transporter-mediated uptake of AEA via a selective “anandamide membrane transporter,” a few papers recently proposed that the transport occurs by simple diffusion or endocytosis via caveolae/lipid rafts Glaser et al., 2005; McFarland et al., 2004a). As a matter of fact, the lack of cloning and expression of the purported transporter protein has prevented the development of molecular tools like oligonucleotides or antibodies, which are able to give definitive proof of the presence of a true transporter on the cell surface. In the same line, AEA analogs able to visualize AEA movement across the plasma membrane and its subsequent fate within the cell, are still missing.

We synthesized and characterized a biotinylated analog of AEA (b-AEA) that has the same lipophilicity of the parent compound. We used

biochemical assays and fluorescence microscopy employing b-AEA as a tool to visualize accumulation, intracellular distribution and trafficking of AEA inside the cells. We chose to modify the polar head of AEA because this structural change does not influence the kinetics of AEA uptake (Piomelli et al., 1999). We used human keratinocyte cells (HaCaT) and human neuronal SH-SY5Y because they have a full and functional endocannabinoids system (Maccarrone et al., 2003a; Pasquariello et al., 2009) and are suitable for immuno-microscopy studies (Maccarrone et al., 2003a).

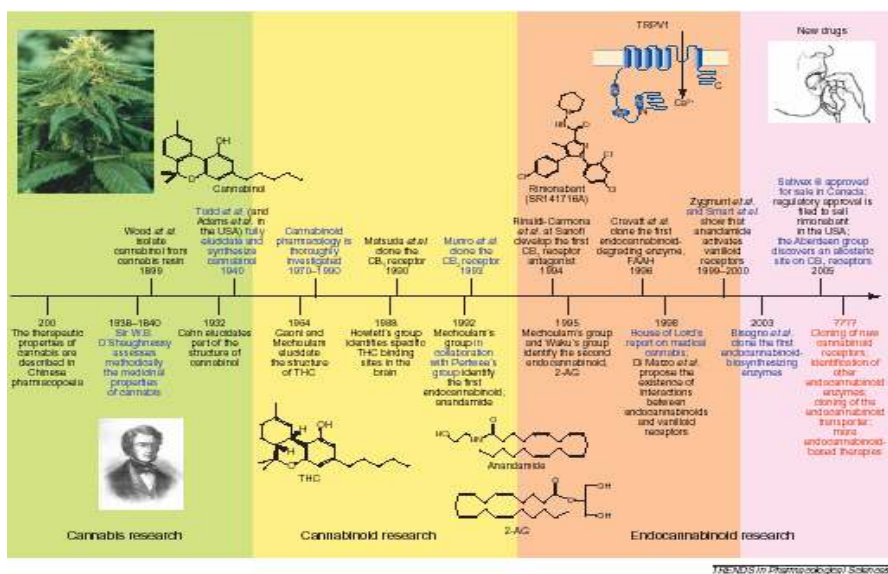


Figure 1. Major breakthroughs in the recent history of cannabis, cannabinoid and endocannabinoid research.

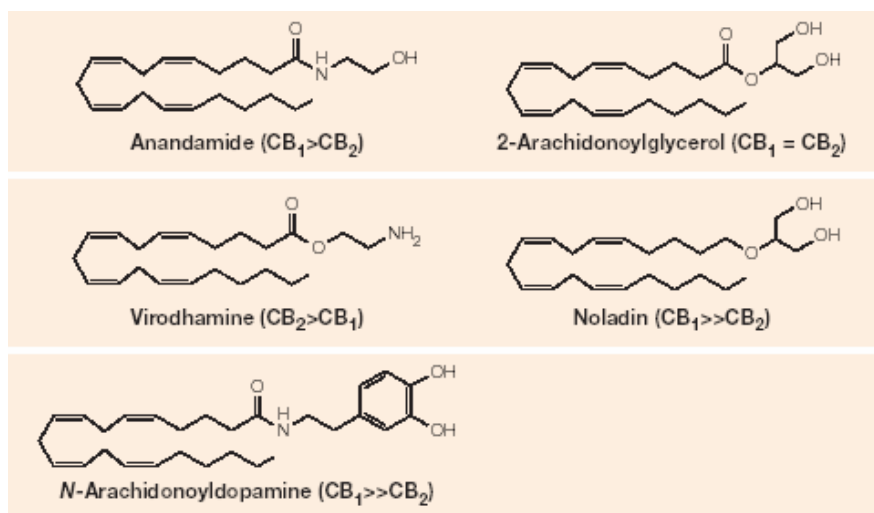


Figure 2. Chemical structures of endocannabinoids and putative endocannabinoids

CHAPTER 1. THE ENDOCANNABINOID SYSTEM

1.1 Molecular targets

AEA and the other endocannabinoids act at first binding or interacting with cannabinoid receptors. The most important of them are CB1 and CB2 receptors (Pertwee and Ross, 2002). There is some evidence that endocannabinoids induce a biological activity via other CB receptors, like a purported CB3 (GPR55) receptor (Sawzdargo et al., 1999; Backer et al., 2006; McPartland et al., 2006; Ryberg et al., 2007), via non-CB1/non-CB2 receptors, or via non-cannabinoid receptors. In the latter group, transient receptor potential vanilloid 1 (TRPV1) has emerged as an important target of AEA, but remarkably not of 2-AG. Moreover AEA can act on a members of nuclear receptor superfamily, the peroxisome proliferator-activated receptors- γ (PPAR γ) (Bouaboula et al., 2005).

Type-1 cannabinoid receptor (CB1) and type-2 cannabinoid receptor (CB2) are seven trans-membrane spanning receptors. The CB1R, cloned in 1990 (Matsuda et al., 1990), is expressed highly in those regions of the brain that correlate with the observed effects of cannabinoids impairment in cognition, memory and motor coordination. Hence, CB1R have been isolated in hippocampus, basal ganglia, cerebral cortex, amygdala and cerebellum (Glass et al., 1997). In the periphery the CB1R has been identified in the pituitary gland, immune cells reproductive tissues, gastrointestinal tissues, sympathetic ganglia, heart, lung, urinary bladder and adrenal gland (Galiegue et al., 1995).

The CB2R was cloned from human promyelocytic leukaemia cells (HL-60 cells) (Munro et al., 1993). It has 68% of amino acid sequence homology to the CB1 receptor within the transmembrane domains and only 44% of homology throughout the total protein (Munro et al., 1993) (Fig. 3). The CB2 receptor is restricted to the periphery where it has been observed in the spleen (Munro et al., 1993, Schatz et al., 1997), in tonsils and on immune cells (B-cells, monocytes, T-cells) (Munro et al., 1993, Galiegue et al., 1995, Schatz et al., 1997). Yet, it has been found in the retina of adult rats (Lu et al., 2000) and it can be expressed in brain microglial cells (Franklin and Stella, 2003).

Other data suggest the presence of novel, uncloned cannabinoid receptors. Using the brains of CB1 knockout mice (CB1^{-/-}) it was shown that there was significant binding of the cannabinoid agonist [3H]WIN 55,212-2 (Breivogel et al., 2001). Moreover, both WIN55,212-2 and the endogenous cannabinoid anandamide were still able to stimulate some labelled non-hydrolysable GTP ([35S]GTPγS) binding in CB1^{-/-} brain, an indicator of GPCR activation. This effect was not blocked by the CB1 receptor antagonist SR141716 (Breivogel et al., 2001). These data are supported by the observation that three typical cannabimimetic effects of AEA, the inhibition of spontaneous activity in an 'open field', the induction of immobility on a 'ring' and the antinociception in the 'hot plate' test, can still be observed in transgenic mice lacking the CB1 receptor (Di Marzo et al., 2002)

More results obtained from experiments with tissues containing naturally expressed cannabinoid receptors and with cells that have been transfected with CB1 or CB2 receptors indicate that both these receptor types can couple through Gi/o proteins.

The first characterised CB1 receptor signal transduction response was the inhibition of adenylyl cyclase by micromolar concentrations of Δ⁹-THC in N18TG2 neuroblastoma cells (Howlett and Fleming, 1984). This response was blocked by pertussis toxin (PTX) suggesting the involvement of Gi/o proteins (Howlett et al., 1986).

The CB1 receptor can interact with Gs under conditions of PTX treatment that prevents the receptor's interaction with Gi/o proteins. (Howlett et al., 1986). Since nine distinct isozymes of adenylyl cyclase have been identified, categorised into six distinct classes based on sequence and functional similarities (Patel et al., 2001), it is possible that the dual coupling of cannabinoid receptors to Gs and Gi/o and so the contrasting effects of cannabinoids on adenylyl cyclase activity, could be attributed to the specific isoform present in different cellular preparations. CB1 receptors have been shown to link positively to mitogen-activated protein kinase (MAPK). In CHO cells, expressing CB1 receptors, the cannabinoid agonist CP 55,940 activated a p42/p44 MAP kinase (Galve-Roperh et al., 2002). These effects were PTX- and SR141716-sensitive (Bouaboula et al., 1995).

CB1 receptors are also coupled through Gi/o proteins to ion channels, positively to A-type and inwardly rectifying potassium channels and negatively to N-type and P/Q type calcium channels and to D-type potassium channels (Pertwee, 1997; 2001; Howlett and Mukhopadhyay, 2000). In addition, there is evidence that CB1 receptors are negatively coupled to

postsynaptic M-type potassium channels in rat hippocampal CA1 pyramidal neurons and to voltage gated L-type calcium channels in cat cerebral arterial smooth muscle cells and in retinal bipolar cell axon terminals of larval tiger salamanders (Pertwee, 2001; Howlett and Mukhopadhyay, 2000).

Similar to CB1, CB2 receptors can modulate adenylyl cyclase and MAPK activity through their ability to couple to Gi/o proteins (Felder et al., 1995; Kobayashi et al., 2001). However, in contrast to CB1, CB2 receptor stimulation is believed not to modulate ion channel function, as seen in AtT-20 cells transfected with CB2 receptors (Felder et al., 1995) and *Xenopus* oocytes transfected with CB2R and GIRK1/4 (McAllister et al., 1999).

A number of investigations have demonstrated the ability of anandamide to activate the TRPV1 receptor (Fig. 4), although it is thought to do so by binding to sites on the cytosolic side of the receptor (De Petrocellis et al., 2001).

TRPV1 is a six trans-membrane spanning protein with intracellular N- and C-terminals and a pore-loop between the fifth and sixth transmembrane helices (Jung et al., 1999). This ligand-gated and non-selective cationic channel is activated by molecules derived from plants, such as the pungent component of 'hot' red peppers capsaicin, by noxious stimuli like heat and protons (Jordt and Julius, 2002) [38] and by peptides contained in spider toxins (Siemens et al., 2006) [39]. Also AEA is considered a true 'endovanilloid' (van der Stelt and Di Marzo, 2004; Starowicz et al., 2007), that behaves as an authentic (though weak) ligand of TRPV1. It evokes vascular relaxation in arteries of the guinea-pig, in a capsazepine-sensitive manner (Zygmunt et al., 1999), indicating that AEA could activate TRPV1 channels in physiological preparations. This response could not be attributed to cannabinoid receptors because neither WIN 55,212-2 nor HU-210 were able to evoke the response while SR141716 failed to attenuate the vasodilatory actions of anandamide. Anandamide has also been shown to activate TRPV1 receptors in rat hippocampal slices (Al-Hayani et al., 2001).

One activity of AEA that has attracted interest is its ability to induce apoptosis in neuronal and peripheral cells (Maccarrone and Finazzi-Agrò, 2003b). This observation could have therapeutic potential in cancer (Guzman, 2003) and neurodegenerative diseases (Cravatt and Lichtman, 2003; Piomelli, 2003). In a previous study we have shown that the pro-apoptotic activity of AEA occurs through activation of TRPV1 (Maccarrone et al., 2000a). We showed that AEA is a physiological agonist of TRPV1 (De Petrocellis et al., 2001) so can be also considered a true endovanilloid (van der Stelt and Di Marzo, 2004). But activation of CB1R protects cells

against AEA-induced apoptosis, suggesting that vanilloid and cannabinoid receptors regulate in opposite ways the apoptotic potential of AEA (Maccarrone et al., 2000a; Yamayi et al., 2003)

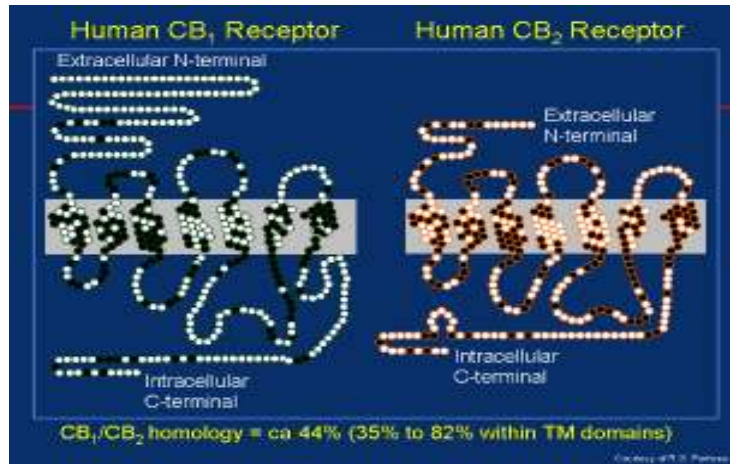


Figure 3. Schematic representation of cannabinoid receptors and their homology

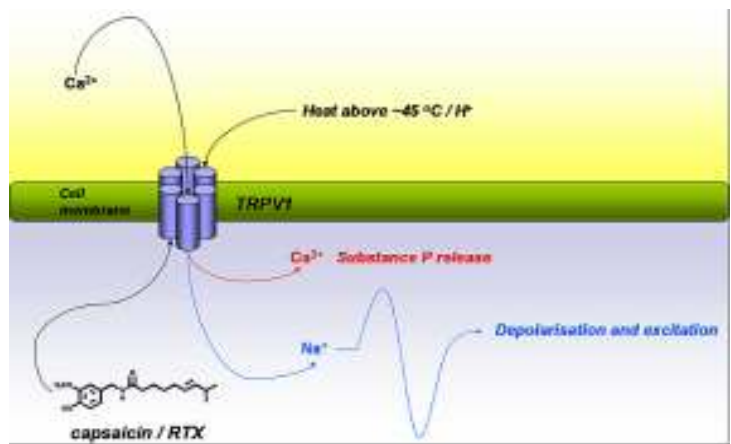


Figure 4. Schematic representation of vanilloid receptor TRPV1

1.2 AEA metabolism

1.2.1 AEA biosynthesis

AEA was originally isolated from porcine brain as the first endogenous cannabinoid (Devane et al., 1992). Ligand binding studies have suggested that it can act at both the CB1 (K_i 61 nM) and the CB2 (K_i 1930 nM) receptors, although it may be more efficacious at CB1 (Felder et al., 1995). AEA behaves as an affinity-driven CB1 receptor agonist. Thus its efficacy at CB1 receptors, although higher than that of Δ⁹-THC, is often found to be lower than those of other cannabinoid agonists [e.g., (+)-WIN55212-2 or CP-55940]. AEA biosynthesis has been demonstrated in neurons (Di Marzo et al., 1994), macrophages (Di Marzo et al., 1996b), and many other tissues and cell types. Unlike other mediators, this compound is not stored in secretory vesicles but is formed “on demand” in a Ca²⁺-dependent manner (Di Marzo et al., 1994) and in a two-step process: (i) first the N-acylation of phosphatidylethanolamine (PE) by an acyltransferase named NAT, generates N-arachidonoyl-phosphatidylethanolamine (NArPE), (ii) then an hydrolase converts NArPE into AEA.

(i) In the first step, NAT catalyzes direct transfer of arachidonic acid from the *sn*-1 position of phosphatidylcholine (PC), generating N-arachidonoylphosphatidylethanolamine (NArPE), the AEA precursor. This biosynthetic pathway is in agreement with the observation that AEA levels are lower than those of the other NAEs in most of the tissues analyzed because the arachidonic acid levels in position 1 of phospholipids are very low. (ii) In the last step NArPE is hydrolyzed by NAPE-PLD which releases AEA and phosphatidic acid (PA). This enzyme has been cloned and purified from rat heart and classified as a member of the zinc metallo-hydrolase family of the β-lactamase fold (Okamoto et al., 2004). NAPE-PLD does not recognize phosphatidylcholine and phosphatidylethanolamine as substrates, and it is widely distributed in mouse organs with highest concentrations in brain, kidney and testis (Okamoto et al., 2004). The same group who characterized NAPE-PLD also suggested that several PLA1/A2 isozymes can generate N-arachidonoyl-lysoPE (NAr-lysoPE) from NArPE, and that a lysoPLD may release AEA from NAr-lysoPE. Therefore, the sequential

action of PLA1/A2 and lysoPLD may represent an alternative biosynthetic pathway for NAEs, including AEA (Sun et al., 2004).

The wide distribution of NAPE-PLD in various brain regions further supports its central role in the formation of AEA and other N-acylethanolamines in the CNS (Morishita et al., 2005).

However, two more mechanisms have been recently described to occur in macrophages and brain homogenates, respectively, for the transformation of NArPE into AEA (Starowicz et al. 2007): (i) the phospholipase C-dependent conversion to phospho-AEA, followed by the hydrolysis of the latter to AEA by PTPN22, a tyrosine phosphatase enzyme (Liu et al., 2006) and (ii) the action of alpha/beta-hydrolase 4 (Abh4) as a lysophospholipase/phospholipase B for the formation of glycerol-phospho-AEA, which is then converted into AEA by an as-yet-unidentified phosphodiesterase (Simon and Cravatt, 2006) (Fig. 5A).

1.2.2 AEA degradation and uptake

As a putative neuromodulator, AEA that is released into the synaptic cleft is expected to be rapidly inactivated. In general, two mechanisms are known to remove endocannabinoids from the synaptic cleft to ensure rapid signal inactivation: re-uptake mediated by a putative transporter that promotes the cellular uptake of AEA (AMT) (Fig. 6) or enzymatic degradation by fatty acid amide hydrolase (FAAH) which hydrolyzes AEA to arachidonic acid and ethanolamine. Whereas the role of FAAH in AEA metabolism is well characterized, the existence of the putative AEA membrane transporter remains controversial. Since AEA is a lipophilic compound, it can diffuse passively through lipid membranes and this process can be accelerated by a rapid and selective mechanism, both in neurons and glial cells (Di Marzo et al., 1994; Beltramo et al., 1997; Hillard et al., 1997). Although Glaser et al. (2003) proposed that AEA cellular uptake is facilitated uniquely by the intracellular hydrolysis by FAAH, other studies (Ligresti et al. 2004, Fegley et al. 2004) using preparations from FAAH null mice, demonstrated that FAAH alone does not account for the facilitated diffusion of AEA across the cell membrane. That at least one protein different from FAAH is required to facilitate AEA transport across the plasma membrane in a selective and bidirectional way was also indirectly suggested by the fact that AEA uptake (and possibly its release) can be stimulated by NO (Maccarrone et al., 1998) and blocked by selective inhibitors (De Petrocellis et al., 2001; Lopez-

Rodriguez et al., 2003; Ortar et al., 2003; Ligresti et al., 2004) with no concomitant effect on FAAH. However, the elusive nature of the putative protein responsible for endocannabinoid transport across the plasma membrane initiated a discussion that is still debating (Hillard and Jarrahian, 2003). After internalization, AEA is hydrolyzed to arachidonic acid and ethanolamine by FAAH, an intracellular membrane-bound serine hydrolase (Hillard et al., 1995; Ueda et al., 1995a). This enzyme was cloned in 1996 (Cravatt et al., 1996) and its X-ray structure has been characterized in detail a few years later (Bracey et al., 2002). FAAH is mainly expressed in microsomal membranes and has an alkaline optimal pH. Extensive SAR studies for the interaction of fatty acid long chain derivatives with FAAH have been reported suggesting that both the alkyl chain and the polar “head” of AEA are important for interaction with the active site. Another amidase, seemingly located in lysosomes, and playing a major role in the inactivation of the AEA congener, N-palmitoyl-ethanolamine, has been also characterized (Ueda et al., 2001). FAAH is widely distributed in the rat brain, where it is expressed at high concentrations in cell bodies and dendrites of several neurons (Tsou et al., 1998; Egertova et al., 2003). Interestingly, in brain areas such as hippocampus, neocortex and cerebellum, FAAH-immunoreactive (ir) cell bodies are exposed to CB1-positive axon terminals, indicating that FAAH not only regulates inactivation of AEA but also that this process is mostly postsynaptic (Fig. 6). Since AEA activates TRPV1 by acting at an intracellular site, its degradation by FAAH should limit its activity at this target (De Petrocellis et al., 2001).

Recent proteomic data suggest the existence of a second mammalian AS enzyme with FAAH activity, called FAAH-2 (Wei et al., 2006). The FAAH-2 gene was found in primates and in distantly related vertebrates but not in rodents like mice and rats. This enzyme exhibits an overlapping but distinct tissue distribution, substrate selectivity, and inhibitor sensitivity compared to the original FAAH enzyme. Both FAAH-1 and FAAH-2 share 20% amino acid sequence identity. Comparison of the enzymatic properties of FAAH-1 and FAAH-2 revealed that FAAH-1 has much higher hydrolytic activity than FAAH-2, with AEA (C20:4) as substrate. This differential activity contrasted with the similar rates of hydrolysis displayed by the two enzymes with oleamide (C18:10) and linoleamide (C18:1) FAAs. FAAH-2 thus appears to prefer monounsaturated over polyunsaturated acyl chains, while FAAH-1 exhibits the opposite selectivity. These observations indicate that FAAH-2 may be important for the regulation of monounsaturated lipid

amides in the CNS and peripheral tissues; however, further investigation is needed (Wei et al., 2006).

In addition to its hydrolysis by FAAH, AEA is metabolized by COX-2, lipoxygenase (LOX) and cytochrome P450 (Fig. 5B). COX-2 has been shown to metabolize AEA into PGE₂-ethanolamide (PGE₂-EA) (Ross et al., 2002). 12- and 15-LOX, non-heme iron-containing enzymes convert AEA into 12- and 15-hydroxy-AEA (12- and 15-HAEA) in vitro, respectively (Kozak et al., 2002; Ueda et al., 1995b). Cytochrome P450 also metabolizes AEA into several polar lipids (Burstein et al., 2000). cDNA cloning and functional expression of the enzyme termed “N-acylethanolaminehydrolyzing acid amidase (NAAA)” from human, rat, and mouse has been reported and had no homology to FAAH but belonged to the choloylglycine hydrolase family (Tsuboi et al., 2005). NAAA was revealed to be a glycoprotein localizing mainly in lysosomes (Tsuboi et al., 2005). Recently, in the absence of FAAH, exogenously injected AEA was shown to be converted into o-phosphorylcholine (o-PC)-AEA in the brain and spinal cord. The choline-specific phosphodiesterase (NPP6) was found to convert PC-NAE into NAE (Mulder and Cravatt, 2006). Further research is required to elucidate the exact mechanism and enzymes involved in this pathway of AEA metabolism.

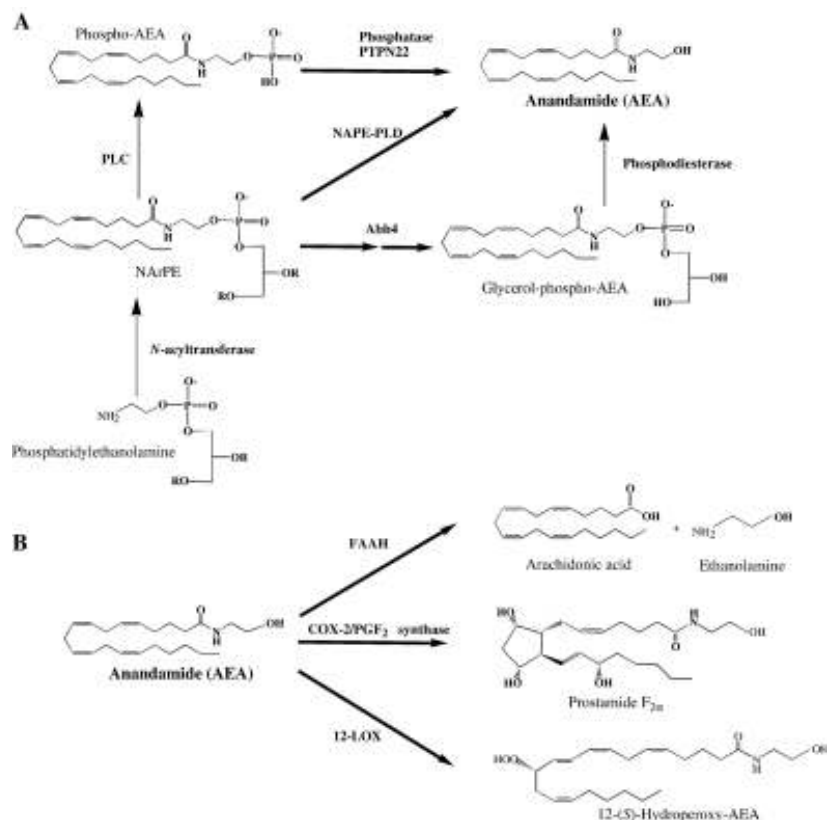


Figure 5. Biochemical pathways for AEA biosynthesis (A) and metabolism (B).

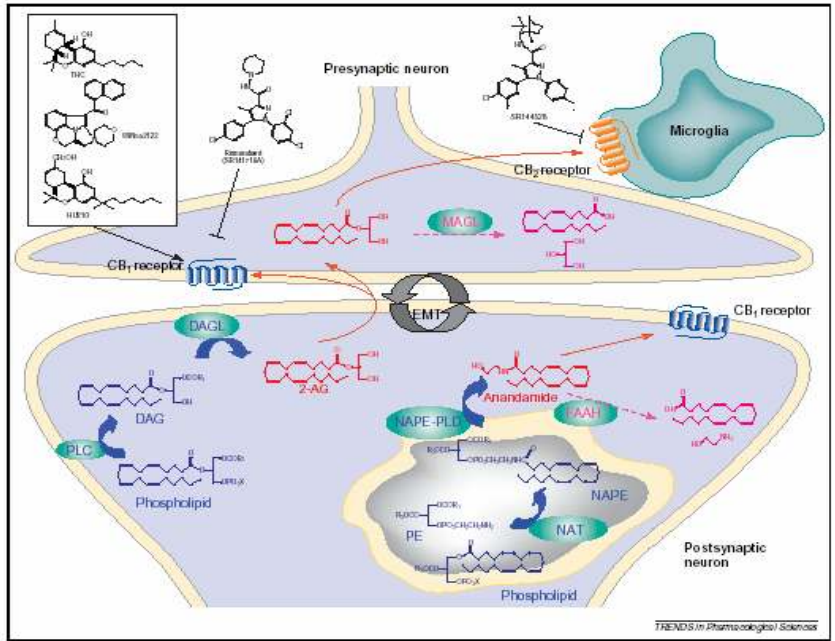


Figure 6. Representation of the Endocannabinoid System in the brain

1.3 2-AG metabolism

1.3.1 2-AG biosynthesis

2-AG has been characterized as a unique monoacylglycerol species isolated from the canine gut (Mechoulam et al., 1995) and rat brain (Sugiura et al., 2000) and as an endogenous cannabinoid receptor ligand. According to its chemical structure, this endocannabinoid is an arachidonyl ester rather than an amide (Basavarajappa et al., 2007; Basavarajappa et al., 2006; Howlett et al., 2002); it was found to bind to both CB1 (K_i 2.4 μM) and CB2 receptors. The CB1 receptor binding activity of 2-AG was 24-times less potent than that of AEA. 2-AG caused the typical effects of Δ⁹-THC, such as antinociception, immobility, immunomodulation, and inhibition of electrically evoked contractions of the mouse vas deferens (Mechoulam et al., 1995; Sugiura et al., 1996; Sugiura et al., 1995). The levels of 2-AG in tissue and cells are usually much higher than those of AEA and are sufficient in principle to activate both cannabinoid receptor subtype (Sugiura et al., 1995).

2-AG biosynthesis occurs by two possible routes in neurons. Phospholipase C (PLC)-mediated hydrolysis of membrane phospholipids may produce diacylglycerol (DAG), which may be subsequently converted to 2-AG by a *sn*-1-DAG lipase (Stella et al., 1997; Bisogno et al., 2003). Alternatively, phospholipase A1 (PLA1) may generate a lysophospholipid, which may be hydrolyzed to 2-AG by lyso-PLC activity (Sugiura et al., 1995). LysoPI-specific PLC is distinct from various other types of PLCs that act on other inositol phospholipids and is located in the synaptosomes (Tsutsumi et al., 1994; Ueda et al., 1993a; Ueda et al., 1993b). Under certain conditions, 2-AG can also be synthesized through the conversion of 2-arachidonyl lysophosphatidic acid (LPA) by a phosphatase to yield 2-AG (Nakane et al., 2002).

Two *sn*-1-specific DAG lipases responsible for the synthesis of 2-AG have been cloned by comparing human genome with *Penicillium* DAGL sequence (Bisogno et al., 2003). Both proteins were found to have four transmembrane domains, and are members of the serine-lipase family with Ser443 and Asp495 participating in the enzymatic catalytic triad. DAGLα (120 kDa) and β (70 kDa) have shown an optimum at pH 7 and are

differentially regulated in the brain depending on the area. For example during the embryonic development they facilitate axonal growth (Williams et al., 2003). In addition the α isoform seems to be predominant in the adult brain, while the β isoform is expressed in developing brain (Bisogno et al., 2003).

DAGL appears to be targeted to postsynaptic spines; it is highly enriched at the base of the spine neck and in the adjacent somatodendritic membrane but is excluded from the main body of the spines and the excitatory synapses in cerebellar Purkinje cells. In hippocampal pyramidal cells, DAGL is distributed at the spine head or neck or at both structures (Katona et al., 2006; Yoshida et al., 2006). The different localizations in different neuron types suggest that the specificity and efficiency of endocannabinoid-mediated retrograde suppression of neurotransmission depend not only on CB1 expression levels in presynaptic elements but also on the distance between the postsynaptic site of 2-AG production and the presynaptic CB1 receptor.

Recently, it has been demonstrated that in primary cultures of mouse microglial cells and astrocytes, millimolar concentrations of ATP significantly increase 2-AG synthesis without acting on AEA production. ATP enhances 2-AG levels in a time-dependent manner by activating purinergic P2X7 receptors (Witting et al., 2004). These ionotropic receptors are permanently permeable to Ca^{2+} (James and Butt, 2002), confirming the relevant role of calcium in the biosynthesis of endocannabinoids (Stella and Piomelli, 2001). Interestingly DAGL activity may be enhanced in peripheral systems by the potent bioactive phospholipid, platelet-activating factor (PAF) (Berdyshev et al., 2001).

1.3.2 2-AG degradation and uptake

It has been suggested that 2-AG can be re-uptaked by the same transporter used by anandamide, i.e. AMT (Beltramo and Piomelli, 2000; Bisogno et al., 2001) (Fig. 7). Human astrocytoma cells, like primary neuronal cell cultures, have been shown to accumulate radioactive 2-AG through an Na^{+} - and ATP-independent process (Hajos et al., 2004). This accumulation is tightly temperature- and concentration- dependent and is reduced by AM404 (N-(4-hydroxyphenyl)-arachidonamide), an AMT inhibitor, and indirectly by high concentrations of arachidonic acid (Beltramo and Piomelli, 2000). The effect

of AM404 is due to the inhibition of AMT and not to the blocking of FAAH activity, because using two strong FAAH inhibitors like URB597 and AM374, the concentration of 2-AG remained unaltered (Hajos et al., 2004).

Once inside the cell 2-AG is degraded. Although FAAH can catalyze 2-AG hydrolysis (Di Marzo and Deutsch, 1998), its levels are not increased in FAAH “knockout” mice, unlike those of AEA (Lichtman et al., 2002). This observation is in agreement with the previously reported evidence regarding the existence of other enzymes catalyzing 2-AG inactivation different from FAAH (Di Marzo et al., 1999; Goparaju et al., 1999). 2-AG is predominantly degraded by monoacylglycerol lipase (MAGL) in the same manner as other monoacylglycerols (Konrad et al., 1994). A MAG lipase, inactive on AEA and with high homology with other human and mouse MAGLs, has been cloned from human, mouse and rat (Karlsson et al., 2001; Ho et al., 2002; Dinh et al., 2002). In rat brain, this MAGL is present with the highest levels in regions where CB1 cannabinoid receptors are expressed (hippocampus, cortex, anterior thalamus and cerebellum). Furthermore, immunohistochemical studies in the hippocampus suggested a presynaptic localization of the enzyme, supporting the role of rat MAGL in the degradation of 2-AG as retrograde messenger, and supplementing the data showing that the DAGLs responsible for 2-AG production are instead postsynaptic in the adult brain (Dinh et al., 2002; Bisogno et al., 2003). Recent studies have confirmed the complementary localization in the brain for the MAGL and FAAH, pre-synaptic and post-synaptic, respectively, suggesting different roles for the two endocannabinoids in the CNS (Gulyas et al., 2004). 2-AG is metabolized to 2-arachidonyl LPA through the action of monoacyl glycerol kinase(s). 2-Arachidonyl LPA is then converted into 1-steroyl-2-arachidonyl PA (Simpson et al., 1991). 1-Steroyl-2-arachidonyl PA is further utilized in the “PI cycle” or is used in the de novo synthesis of phosphatidylcholine (PC) and phosphatidylethanolamine (PE). Furthermore, 2-AG is metabolized by enzymatic oxygenation by cyclooxygenase-2 (COX-2) into prostaglandin H₂ (PGH₂) glycerol esters. The biological activity and the role of oxygenated 2-AG have yet to be determined. Inhibition of COX-2 prolongs DSI, suggesting that COX-2 limits endocannabinoid action in retrograde signaling and synaptic plasticity (Kim and Alger, 2004; Sang et al., 2006; Slanina et al., 2005).

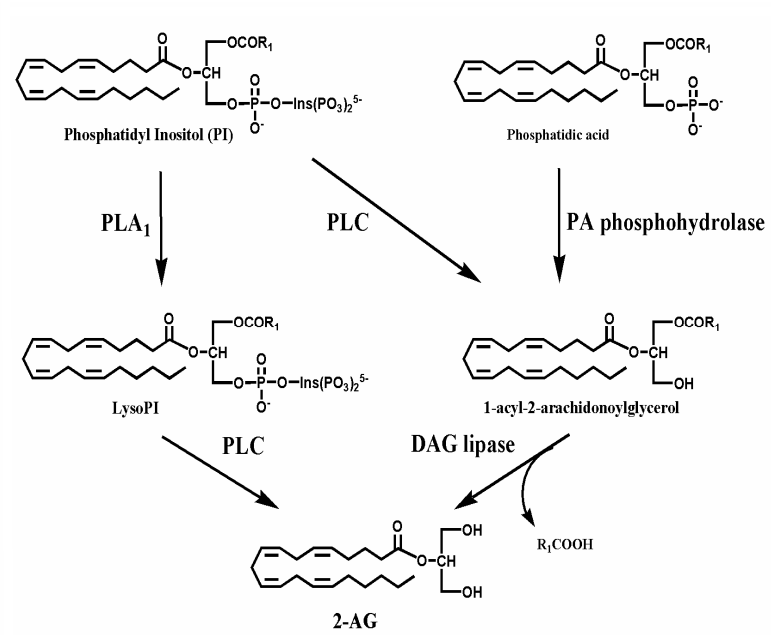


Figure 7. Biochemical pathways for 2-AG biosynthesis

CHAPTER 2. FLUORESCENT LIPID PROBES

Cells contain an enormous variety of biomolecules. The concentrations, chemical modifications and interactions of these molecules are generally precisely controlled, both spatially and temporally. Deciphering this complex system of interacting molecules inside and among the cells is one of the final goals of biology (Terai, 2008).

Fluorescence based on small organic compounds used as probes themselves or on modification of cellular molecules that can be tied to fluorescent proteins, has become an important tool in modern biology because it allows to have informations about localization and quantity of the molecules of interest. All without the need of genetic engineering of the sample.

Compared to other technologies like radioisotope labelling, fluorescence imaging has many advantages for this purpose, as it enables highly sensitive, non-invasive, and safe detection using readily available instruments. Another advantage of fluorescence imaging is that the fluorescence signal of a molecule can be modulated, so that sensors relying on ‘activation’, not just accumulation, can be utilized. Until the 1980s, however, fluorescence imaging was mainly applied to fixed samples owing to the lack of fluorescent chemosensors, or probes, suitable for imaging in living cells (Terai, 2008).

In lipid research, the last two decades of the previous century were highlighted by rapid developments in the recognition of the role of lipids in a great variety of cellular processes, ranging from membrane fusion, involvement in microdomain formation and transport, to signal transduction (Hoekstra et al., 1994). So they were elevated from only dangerous dietary molecules to essential compounds of body’s health and function.

Lipids are amphiphilic in nature and consist of a hydrophobic chain and a hydrophilic head group region. So there are in principle two regions within the molecule to which fluorescent dyes can be covalently coupled. The intramolecular localization of the dye as well as the chemical nature of the dye itself (Fig. 8) are highly relevant: they will determine the (biophysical) properties of the final fluorescent lipid and subsequently the

assay in which the probes will be used. The majority of the fluorescent dyes that have been used in lipid derivatization, especially those emitting in the visible light region, are hydrophilic. When they are attached in the chain region, the dye will change the hydrophilic/hydrophobic balance of the lipid molecule. Evidently, such a perturbation may have considerable implications for the lipid's ability to integrate into membranes (Maier et al., 2002) and to interact with the proteins of interest. Histochemistry is the microscopical study of the distribution of substances in tissues using chemical reactions that generate visible products. In the middle years of the twentieth century many histochemical methods were devised for localising enzymatic activities in cells and tissues. Typically, a section of tissue is incubated with an artificial substrate for the enzyme. A product of the enzyme-catalysed reaction is immediately trapped by reaction with another compound in the incubation medium, generating a visible product that either is insoluble or binds firmly to the structural proteins of the cell. Because enzymes are catalysts, many molecules of visible product are produced by each molecule of enzyme in a histochemical reaction. This is a form of amplification. Some enzymes are used as reagents to amplify the histochemical detection of many substances in tissues (Kiernan, 2006). An example is given by the strong and specific affinity of biotin for avidin (Guesdon et al., 1979) or streptavidin. Biotin, a vitamin synthesised by microorganisms in the intestine, is not coloured or fluorescent, but it can be localised with great sensitivity and specificity on account of its high affinity for avidin, a basic glycoprotein component of egg white. Streptavidin is a neutral biotin-binding protein produced by *Streptomyces avidinii*. It is not a glycoprotein. Immunostaining methods using avidin sometimes give non-specific background colour; this artefact is less when streptavidin, a more expensive reagent, is used (Kiernan, 2006).

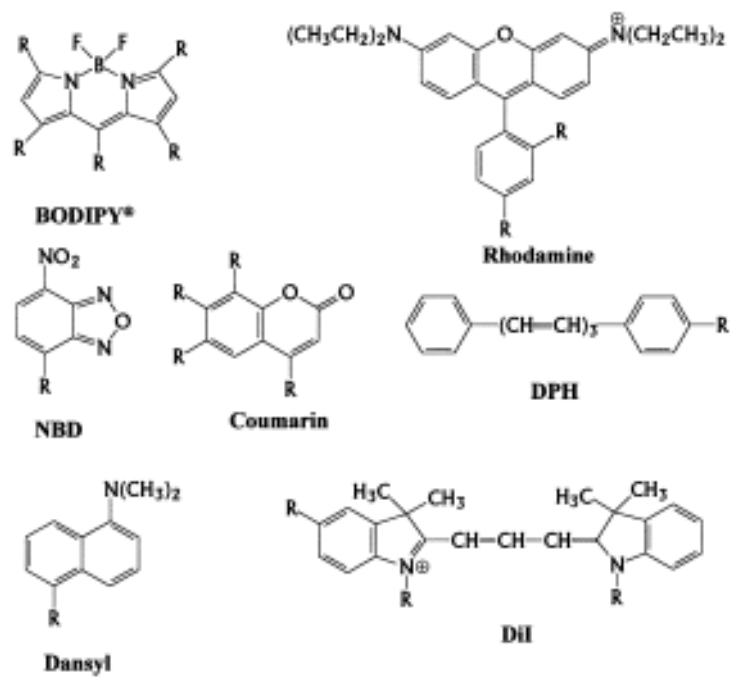


Figure 8. Basic structures of fluorescent dyes used for coupling to lipidic structures. R represents either lipidic anchors or other functional groups.

CHAPTER 3. OBJECTIVES OF THE RESEARCH

The aim of our studies was to characterize a biotinylated analog of AEA (b-AEA) designed to visualize the intracellular accumulation of this endocannabinoid through immunomicroscopy techniques. By means of biochemical assays and morphological analysis we wanted to demonstrate that biotinylation of the polar head of AEA doesn't affect its accumulation by the cells but prevents its interaction with FAAH, NAPE-PLD, CB1R, CB2R and TRPV1.

Moreover, using this tool, we focused our attention on intracellular accumulation, trafficking and protein-binding of AEA, the most important endocannabinoid.

CHAPTER 4. RESULTS

4.1 Characterization of b-AEA

We designed an analog of AEA, the biotin-AEA (b-AEA) that could be a new tool to visualize AEA inside the cells. Since previous studies have indicated that the kinetic parameters of AEA uptake are sensitive to modification of the arachidonate moiety, whereas changes in the ethanolamide region are well tolerated (Muthian et al., 2000; Di Marzo et al., 2004), we synthesized b-AEA in which the biotin tag was attached to the polar head of AEA through a spacer arm (Fig. 9A). The synthetic route of b-AEA allowed us to produce both b-AEA and its tritium-labeled analog ($[^3\text{H}]$ b-AEA) with a yield of $\sim 50\%$. The identity and purity of b-AEA was checked by HPLC-ESI-MS and by ^1H NMR. HPLC ESI-MS was performed with a Waters apparatus (Milford, MA), and ^1H NMR was recorded on a Bruker AM series spectrometer (Rheinstetten, Germany) at 300 K and 300 MHz. Biotin-AEA showed an MS spectrum (Fig. 9B) with m/z 5661.8 $[\text{M}+\text{H}]^+$ and a ^1H NMR (CD_3CN) spectrum (Fig. 9C) with δ : 0.88 (3H, t, J 5.1 Hz), 1.24–1.47 (6H, m), 1.49–1.74 (8H, m), 2.06–2.31 (8H, m, partially under water residual peak), 2.66 (1H, d, J 12.9 Hz), 2.77–2.96 (7H, m), 3.14–3.23 (1H, m), 3.26–3.36 (4H, m), 3.46–3.55 (4H, m), 3.58 (4H, s), 4.18–4.29 (1H, m), 4.40–4.46 (1H, m), 5.26–5.48 (8H, m), 6.51–6.56 (bs, 2H). Interestingly, the addition of the biotin tag did not yield any major change in lipophilicity, expressed as logarithm of the partition coefficient in *n*-octanol/water (LogP in Fig. 10), calculated through the HyperChemTM 6.03 Molecular Modeling System (Hypercube, Inc., Gainesville, FL). Also the analysis of low-energy conformations of AEA and b-AEA showed similar electrostatic potentials on the acyl chain moiety (Fig. 10). These conformations were obtained using molecular mechanics geometry optimization with the AMBER94 force field, followed by single-point calculations (HyperChemTM 6.03), as reported (Dainese et al., 2007).

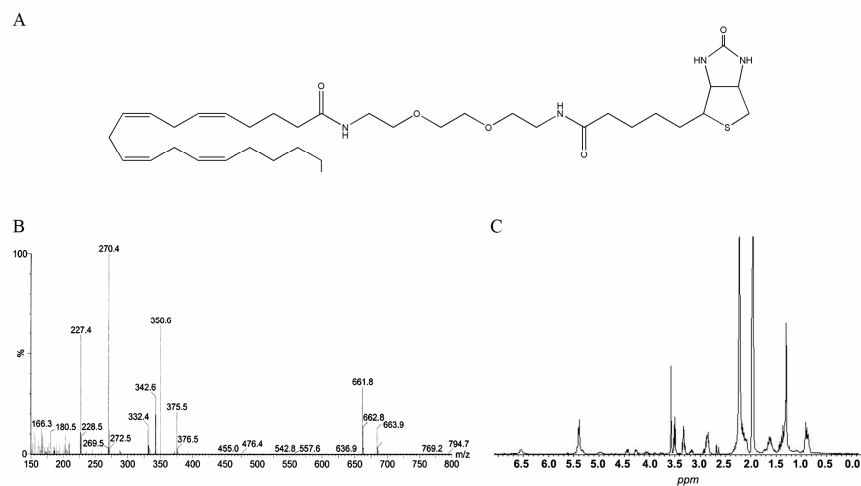


Figure 9. Chemical structure (A), MS spectrum (B), and ¹H NMR spectrum (C) of the biotinylated analog of N-arachidonylethanolamine (b-AEA)

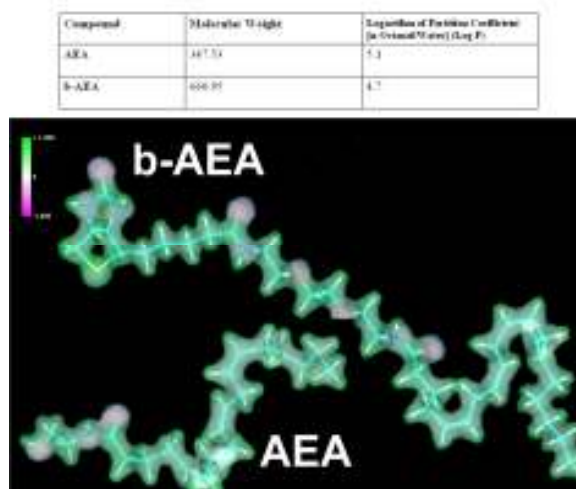


Figure 10. Molecular properties of AEA versus b-AEA. The molecular weight, lipophilicity (LogP), and electrostatic potential of AEA are compared with those of b-AEA. Low-energy conformations of AEA and b-AEA are reported in the bottom panel and show the electrostatic potential on the molecular surface (violet, 21; green, 11).

4.2 Metabolism of AEA and b-AEA in HaCaT cells

We sought to test the similarities in accumulation of AEA and b-AEA in HaCaT cells because they possess a full and functional endocannabinoid system (Maccarrone et al., 2003a) and are suitable for immune-microscopy studies (Oddi et al., 2005). We found that intact HaCaT cells were able to accumulate [3H]b-AEA in a concentration-dependent manner, typical of a saturable process (Fig. 11A). Accumulation of [3H]b-AEA was similar to that of [3H]AEA (Fig. 11A) with apparent K_m and V_{max} values of 421 ± 88 nM and 116 ± 10 pmol/min*mg of protein, respectively (Table 1). These kinetic constants are typical of AEA transport in HaCaT cells (Maccarrone et al., 2003a) as well as in other cell types (Battista et al., 2005; Glaser et al., 2005; Hillard and Jarrahian, 2005). In addition, 5 μ M OMDM-1, a selective AEA uptake inhibitor (Ortar et al., 2003), minimized the uptake of [3H]b-AEA (Fig. 3A) in much the same way as it inhibited that of [3H]AEA in the same cells (Oddi et al., 2005). Unlike [3H]AEA, which was hydrolyzed in a concentration-dependent manner (Fig. 11B) and with kinetic constants (Table 1) typical of FAAH in HaCaT cells (Maccarrone et al., 2003a), [3H]b-AEA was not a substrate for FAAH (Fig. 11B). In particular, we found only intact [3H]b-AEA when we analyzed by RP-HPLC the organic extract of the enzymatic reaction, demonstrating that b-AEA is metabolically stable (data not shown). Furthermore, [3H]b-AEA did not bind to CB1R of HaCaT cells (Fig. 11C), at variance with [3H]AEA, which bound to these receptors (Fig. 11C) with apparent K_d and B_{max} values (Table 1) close to those already found in HaCaT cells (Maccarrone et al., 2003a). Likewise, SR141716 (0.5 μ M), but not SR144528 (0.5 μ M), which are selective antagonists of CB1 or CB2 receptors, respectively (Howlett et al., 2002; Pertwee and Ross, 2002), reduced the binding of 400 nM [3H]AEA to HaCaT cell membranes to ~15% of control values, corroborating previous data (Maccarrone et al., 2003a).

Parameter	Kinetic constant	
	<u>AEA uptake</u>	Km (nM)
AEA	353 ± 60	124 ± 8
b-AEA	421 ± 88	116 ± 10
<u>FAAH</u>	Km (μM)	Vmax (pmol/min per mg protein)
AEA	13 ± 2	385 ± 25
b-AEA	—	—
<u>CB1R</u>	Kd (nM)	Bmax (fmol per mg protein)
AEA	173 ± 38	926 ± 63
b-AEA	—	—

Table 1. Kinetic constants of AEA uptake, FAAH activity, or CB1R binding in HaCaT cells using AEA or b-AEA as substrate or ligand

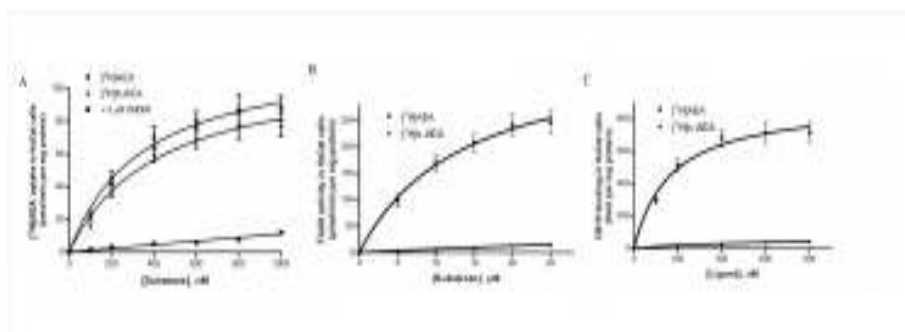


Figure 11. Metabolism of AEA versus b-AEA in HaCaT cells. A: Transport of [3H]AEA and [3H]b-AEA alone. The effect of 5 μM (S)-1'--(4-hydroxybenzyl) oleoylethanolamide (OMDM-1) refers to the uptake of [3H]b-AEA and was superimposable on the effect on the uptake of [3H]AEA (omitted for the sake of clarity). B: Hydrolysis by fatty acid amide hydrolase (FAAH). C: CB1R binding. Error bars represent SD values.

4.3 Inhibition assays of AEA and b-AEA

To further characterize the biochemical profile of biotin-AEA, we performed inhibition assays aimed at calculating the concentration of b-AEA able to reduce by half (IC_{50}) the transport, hydrolysis and biosynthesis of $[3H]AEA$. The results (Table 2) demonstrate that b-AEA does not affect FAAH activity or NAPE-PLD activity of HaCaT cells when used at concentrations up to $10 \mu M$; yet, it does reduce the uptake of $0.5 \mu M$ AEA, with an IC_{50} value of $0.5 \pm 0.1 \mu M$, indicating very similar affinities of the transport machinery toward AEA and its biotinylated derivative (Table 2). We also tested the ability of b-AEA to inhibit the binding of $[3H]CP55.940$, a synthetic agonist of CBRs. To this end, membrane preparations from mouse brain or mouse spleen were used as sources of authentic type-1 and type-2 CB receptors, respectively (Howlett et al., 2002; Pertwee and Ross, 2002). As expected, we detected by Western blot immunoreactivity for CB1R in the mouse whole brain and for CB2R in the spleen; conversely, we did not observe any immunoreactivity for CB1R in the spleen and for CB2R in the brain (data not shown). We also investigated the ability of b-AEA to bind to TRPV1 by performing competition assays with the specific receptor agonist $[3H]RTX$ (Van der Stelt and Di Marzo, 2004; Szallasi et al., 1999). The results (Table 2) demonstrate that b-AEA was inactive toward CB2 or TRPV1 receptors at concentrations up to $10 \mu M$, whereas it was able to inhibit by 50% CB1R binding at $5 \pm 0.7 \mu M$ (Table 2). In order to analyze the interaction of b-AEA with CB1R, we calculated the K_d and B_{max} values for CP55.940 (concentration range, 0–1 nM) in the absence or presence of $10 \mu M$ b-AEA. We found that b-AEA did not affect K_d (720 ± 100 vs. 734 ± 110 pM of controls) but reduced B_{max} almost by half (517 ± 72 vs. 1150 ± 200 fmol/mg of protein of controls). The biochemical data suggest that b-AEA is not a substrate for FAAH, does not interfere with NAPE-PLD, and is not efficiently recognized by the AEA binding receptors. However, b-AEA is transported by the same machinery, and with the same efficiency, as AEA.

Parameter	IC ₅₀ (μM)
Uptake ^a	0.5 ± 0.1
FAAH ^b	> 10
NAPE-PLD ^c	> 10
CB1R ^d	5 ± 0.7
CB2R ^e	> 10
TRPV1 ^f	> 10

Table 2. IC₅₀ values of b-AEA toward uptake, hydrolysis, and biosynthesis of AEA and toward CB1R, CB2R, and TRPV1 binding

Data are means ± SD of three independent experiments.

a Uptake was measured in intact HaCaT cells with 400 nM [3H] AEA as substrate (control=80 ± 9 pmol/min*mg protein).

b Activity was measured in HaCaT cell extracts with 10 μM [3H] AEA as substrate (control=170 ± 18 pmol/min*mg protein).

c Activity was measured in HaCaT cell extracts with 100 μM [3H] N-arachidonoylphosphatidylethanolamine as substrate (control=12 ± 3 pmol/min*mg protein).

d Binding was measured in mouse brain membrane fractions with 400 pM [3H]CP55.940 as ligand (control= 82 ± 8 fmol/mg protein).

e Binding was measured in mouse spleen membrane fractions with 400 pM [3H]CP55.940 as ligand (control= 58 ± 4 fmol/mg protein).

f Binding was measured in C6 cell membrane fractions with 500 pM [3H]resiniferatoxin as ligand (control= 141 ± 22 fmol/mg protein).

4.4 Immunofluorescence studies of b-AEA accumulation

To ascertain whether b-AEA can be used as a probe to visualize the internalization of AEA by intact cells, we next performed immunofluorescence microscopy studies in human HaCaT keratinocytes. b-AEA was detected by indirect immunofluorescence using an anti-biotin monoclonal antibody and an anti-mouse secondary antibody conjugated with a green fluorescent dye. The immunostaining revealed that cells quickly (within 5 min) took up b-AEA, which appeared to accumulate both in the cytosol and in the nucleus (Fig. 12, b-AEA). Interestingly, the biotin tag *per se* was not taken up by the cells under the same experimental conditions (Fig. 12, Ctrl). In line with this, we found that biotinyl-arachidic acid, a saturated analogue of b-AEA, was not transported inside the cells (data not shown), further supporting that it is the arachidonic moiety and not the biotin-tag of b-AEA that is the crucial portion for a correct transport of the molecule across the cell membranes. In addition, we tested the specificity of b-AEA immunostaining in the presence of 5 μM OMDM-1 or 0.1 μM URB597. A remarkable decrease in immunostaining was observed only in HaCaT cells pretreated with OMDM-1, strongly indicating that b-AEA was indeed taken up by a transporter-dependent process (Fig. 12). Instead, the inhibition of FAAH activity by 0.1 μM URB597 did not affect the intracellular accumulation of b-AEA, nor did 0.5 μM SR144528 (Fig. 4) or 10 μM capsazepine, a selective antagonist of TRPV1 (data not shown) (Van der Stelt and Di Marzo, 2004; Szallasi et al., 1999). On the other hand, 0.5 μM SR141716 was able to decrease the fluorescence intensity by ~35% of the control (Fig. 12), indicating a contribution of CB1R to AEA uptake (Oddi et al., 2005; Maccarrone et al., 2000b; Ortega-Gutierrez et al., 2004).

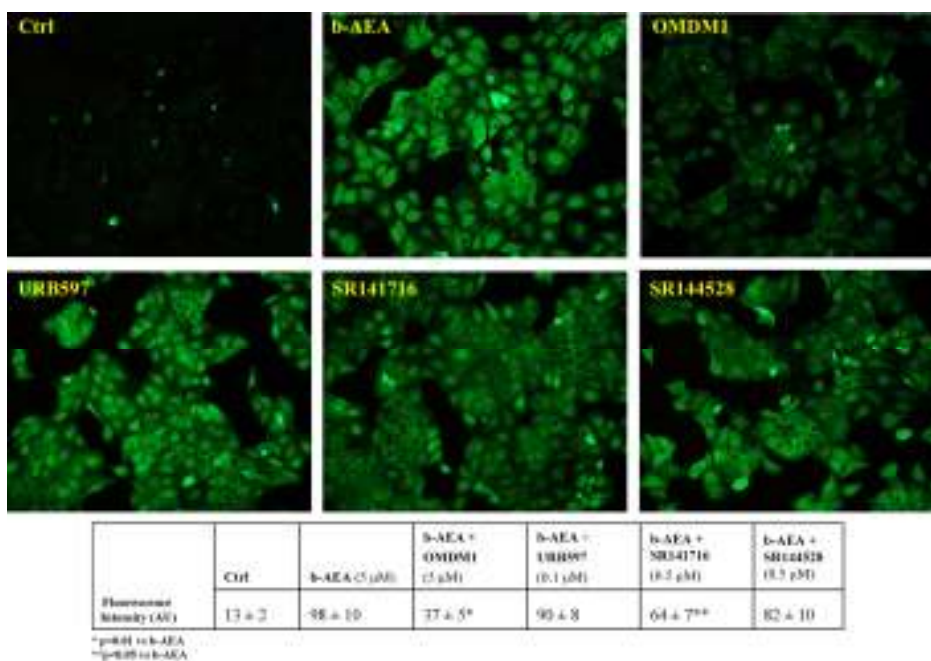


Figure 12. Fluorescence microscopy studies of the distribution of b-AEA in HaCaT cells. No green fluorescence could be detected in negative controls, demonstrating that the biotin tag was not able per se to cross the plasma membrane (Ctrl). Instead, 5 μM b-AEA was internalized, and this process was minimized by 5 μM OMDM-1 and partly by 0.5 μM N-piperidino-5-(4-chlorophenyl)-1-(2,4-dichloro-phenyl)-4-methyl-3-pyrazole carboxamide (SR141716), but not by 0.1 μM cyclohexylcarbamic acid 3'-carbamoyl-biphenyl-3-yl ester (URB597) or 0.5 μM N-[1(S)-endo-1,3,3-trimethyl-bicyclo [2.2.1]heptan-2-yl]5-(4-chloro-3-methylphenyl)-1-(4-methyl-benzyl)-pyrazole-3-carboxamide (SR144528). Images are representative of at least three independent experiments, and five fields were examined for each treatment. Fluorescence intensity (AU, arbitrary units) was quantified by ImageJ software, and values represent means ± 6 SD.

4.5 Visualization of b-AEA accumulation in lipid droplets

We found that once accumulated inside the cells, b-AEA shows a spotted pattern throughout the cytosol with a particular intensity around the nucleus. A considerable part of the vesicular-like staining of b-AEA was associated with cytosolic compartments called lipid droplets (LDs, lipid bodies or adiposomes) (Martin and Parton, 2006). These are cytosolic organelles ubiquitously present in eukaryotic cells, where they act as a storage compartment for neutral lipids (Martin and Parton, 2006). LDs, also called lipid bodies or adiposomes, contain a neutral lipid core of triacylglycerols and sterol esters, and are selectively stained by the phenoxazine dye Nile Red (Gocze and Freeman, 1994). Their lipid core is surrounded by a phospholipid monolayer that interacts with LDs-associated proteins. We found that b-AEA staining was diffused throughout the cytoplasm (Fig. 3A), and that it formed rings surrounding the Nile-Red positive central core of adiposomes (Fig. 13A, inset). These observations suggest that intracellular b-AEA reaches the adiposomes and is stored on their surface. In addition to HaCaT cells (Fig. 13A, inset), b-AEA colocalized with adiposomes also in human neuronal SH-SY5Y cells (Fig. 13D).

To further investigate the functional link between b-AEA and LDs, the dimension of the adiposome compartment was reduced by cell starvation. In fact, the amount of oleic acid present in the medium, and hence the adiposome size, is reduced as a consequence of starvation (Wolins et al., 2001). In serum-starved cells we observed a marked reduction of b-AEA accumulation, which paralleled the reduction of number and size of LDs (Fig. 13C). On the other hand, feeding HaCaT cells with an additional supply of oleic acid considerably increased the uptake of b-AEA, again paralleling the increase in size and number of LDs (Fig. 13B).

4.6 [3H]AEA accumulation in lipid droplets

We confirm the dependence of AEA accumulation on the dimension of LDs by examining the uptake of 400 nM [3H]AEA by HaCaT cells grown with an excess of oleic acid. The net uptake of [3H]AEA in oleic acid-treated cells was approximately threefold higher than that of controls (Fig. 13E). Since the internalization of AEA is thought to be the result of two different processes, i.e., accumulation through saturable intracellular components and FAAH-mediated hydrolysis, we sought to estimate the contribution of AEA hydrolysis by inactivating FAAH with 100 nM URB597 (Kathuria et al., 2003). The enzymatic activity of FAAH in living cells was measured using 400 nM [ethanolamine-1-3H]AEA as substrate under the same conditions used for the assay of AEA transport. The addition of URB597 did not abolish completely FAAH activity, which remained ~40% and ~35% of that of oleate-treated and untreated cells (Fig. 13E, white bars); yet, the partial inhibition of AEA degradation reduced the net uptake of [3H]AEA by ~30% of the controls, both in oleate-treated and untreated cells (Fig. 13E). This observation suggests that FAAH activity, although not a requisite for AEA accumulation, does contribute to this process by maintaining a concentration gradient across the plasma membrane. The contribution of AEA hydrolysis was estimated by the difference between the AEA uptake in the absence and in the presence of URB597, corrected for residual FAAH activity. On this basis, we found that AEA catabolism by FAAH was approximately fivefold faster in oleate-treated cells than in controls, and that the intracellular accumulation of AEA was approximately twofold higher in LDs-enriched cells than in controls (Fig. 13E, hatched bars). These data further indicate that adiposomes are directly involved in the intracellular accumulation of AEA. Since FAAH activity in oleate-treated cell homogenates was comparable to that of controls (122 ± 17 versus 116 ± 10 pmol/min per mg of protein), we also speculated that the higher catabolism of AEA observed in treated cells might be due to a faster shuttling of AEA from plasma membrane to intracellular degradation sites, made possible by adiposomes.

4.7 Morpho-functional overlap between LDs and FAAH

Treating the cells with our tool b-AEA, we found by immunofluorescence experiments that it internalized in HaCaT cells reached the endoplasmic reticulum near the nucleus, where it partially colocalized with FAAH staining (Fig. 13G, yellow arrows in inset). Furthermore, the existence of a morpho-functional overlap between LDs and FAAH was ascertained by co-fractionation studies, which revealed a small but significant amount of FAAH activity associated with adiposome-rich fraction derived from mouse liver (Fig. 13F). Additional colocalization studies revealed that FAAH-positive dots (Fig. 13H, green) were partly associated with the periphery of LDs in HaCaT cells (Fig. 3H, white arrows in inset). Incidentally, these findings confirm the results of a recent proteomic study, which demonstrated the presence of FAAH in purified LDs from *Drosophila* embryos (Cermelli et al., 2006).

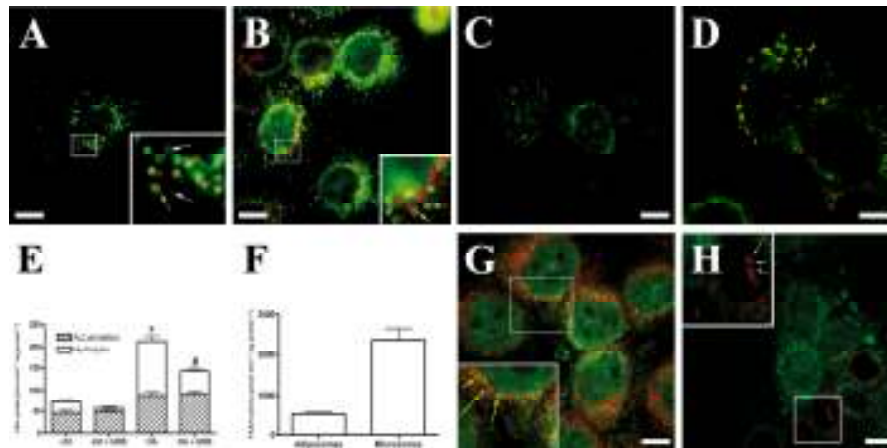


Figure 13. Immunocytochemical localization of b-AEA and FAAH to cytoplasmic lipid droplets (LDs) in human HaCaT cells. (A) LDs in HaCaT cells were stained with Nile Red (red). Cells grown in normal (i.e., low-lipid containing) medium showed colocalization of b-AEA (green) with the rim of the round-shaped lipid bodies (magnified box, yellow arrows). A residual staining seems to be distinct from LDs having a more undefined cytosolic distribution (magnified box; white arrows). (B) Cells treated overnight with 100 μM oleic acid/BSA displayed a significant increase in b-AEA staining, which paralleled the increase of LDs size. (C) Serum-starved cells (i.e., low oleic acid condition) showed a significant reduction of the LDs compartment and a parallel reduction in the accumulation of b-AEA. (D) Immunodetection of b-AEA in SH-SY5Y cells. Images are representative of at least three independent experiments, and five fields were examined for each treatment. (E) Effect of oleic acid treatment (OA) versus control (ctrl) on [3H]AEA uptake by HaCaT cells, grown in the absence or in the presence of 100 nM URB597. In (E), * $p < 0.05$ versus ctrl, and # $p < 0.05$ versus ctrl + URB597 (n=4). (F) Analysis of the FAAH-specific activity in the adiposome fraction and microsomes fraction obtained by mouse liver subfractionation. (G) Co-staining of HaCaT cells with anti-FAAH (green) and anti-biotin (red) antibodies. The superimposition of the two stainings revealed that FAAH and b-AEA colocalize only in dot structures near to the perinuclear region (yellow arrows in the inset). (H) Co-staining of HaCaT cells with anti-FAAH antibodies (green) and Nile red staining for adiposomes (red). The superimposition of the two stainings revealed that several FAAH-positive dots are associated to the periphery of the LDs (white arrows in the inset). Bars, 10 μm.

4.8 Storage of [3H]AEA in adiposome-rich fractions of HaCaT cells

The relationship between AEA and LDs was also investigated by analyzing the intracellular distribution of [3H]AEA after its uptake. We made subcellular fractionation of HaCaT cells grown in the presence of an excess of oleic acid and incubated for 15 min with [3H]AEA. To prevent the degradation of AEA, FAAH was inactivated by preincubating the cells for 10 min with 100 nM URB597. LDs were isolated by flotation (Yu et al., 2000) and characterized by fluorescence staining and Western blotting (Yu et al., 2000). The two top fractions of the gradient (1 and 2), containing only 1% of the total proteins, were positive for adipophilin, an LD-specific protein, and were devoid of markers of caveolae (caveolin-1), endoplasmic reticulum (ER), cytosol (actin) and plasma membranes (Na⁺/K⁺-ATPase) (Fig. 14A). Fluorescence microscopy of Nile Red-stained fractions showed bright, spotted and spherical lipid bodies in all fractions of the gradient, the greatest amount being present in fraction 1 and the smallest amount in fractions 4–8 (Fig. 14B). The distribution of [3H]AEA in these fractions was quantified by radioactivity, normalized to the protein content. We found that the two fractions containing LDs (1 and 2) were also the richest in [3H]AEA (Fig. 14C), further suggesting that adiposomes were important sites for the accumulation of AEA. The [3H]AEA subcellular profile was mirrored by that obtained with [3H]oleic acid, a lipid molecule that is known to specifically accumulate in LDs (Fig. 14D). In addition, to exclude nonspecific associations with LDs, we also analyzed the subcellular distribution of nonyl acridine orange. This fluorescent dye associates with cardiolipin, an anionic phospholipid abundant in mitochondria. As expected, fluorescence of nonyl acridine orange was primarily enriched in the microsomal fraction and was virtually absent from LDs (Fig. 14D). Moreover, by means of radiochromatography we found that ~85% of radioactivity in fractions 1 and 2 was due to intact [3H]AEA whereas only ~15% of radioactivity was [3H]AA (data not shown). To further support the functional interaction between AEA storage, LDs and FAAH, we demonstrated that in the absence of the FAAH inhibitor URB597 the distribution of [3H]AEA markedly changed, with a reduction of radioactivity in the adiposome fraction and a parallel increase in the microsomal fraction (Fig. 14C).

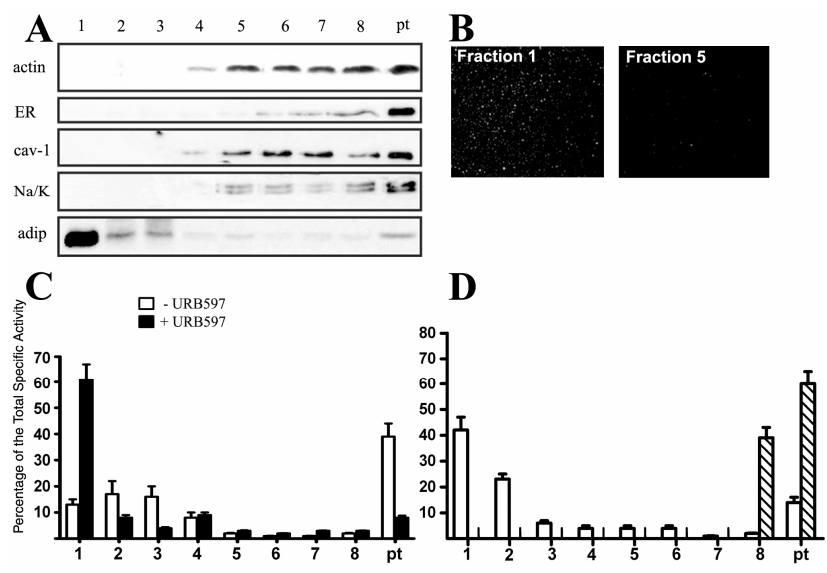


Figure 14. Subcellular distribution of internalized [3H]AEA in human HaCaT cells. (A) The subcellular fractions obtained from HaCaT cells were analyzed by Western blotting using different markers for cytoplasm (actin), endoplasmic reticulum (ER), caveolae (caveolin-1, cav-1), plasma membrane (Na⁺/K⁺-ATPase, Na/K) and lipid droplets (adipophilin, adip). (B) Staining of fraction 1 (LDs) and fraction 5 (cytosol) with Nile Red. (C) Enrichment of [3H]AEA in the subcellular fractions was expressed as percentage of the total specific activity. The radioactivity of accumulated [3H]AEA was measured in the presence (black bars) or in the absence (white bars) of 100 nM URB597 (black bars: 100% = 430 ± 30 dpm/mg protein; white bars: 100% = 1180 ± 50 dpm/mg protein). (D) Content of 3H-labeled oleate (open bars; 100% = 1400 ± 200 dpm/mg protein), and fluorescence of nonyl acridine orange (hatched bars; 100% = 15 ± 20 fluorescence arbitrary units) in subcellular fractions of HaCaT cells.

4.9 Identification of AEA-binding activity within the cytosol

Besides the investigation of the intracellular sites in which AEA could be accumulated, we also tried to explore the presence, within the cytosol, of transporters that could deliver AEA from plasma membrane to internal sites.

In preliminary experiments, we attempted to determine if the epidermal cytosol contained AEA-binding sites. We found that cytosol preparations could bind this endocannabinoid up to about 70 fmol/mg of protein. The protein nature of the AEA-binding sites was indicated by their susceptibility to proteolytic digestion by protease K and their resistance to DNase I, ribonuclease A, and pancreatic lipase (Figure 15A). In order to investigate the specificity of the AEA-binding activity, competitive experiments were performed. Cytosol preparations were incubated with [3H]AEA (2 nM) in the presence of a 50-fold excess of structurally related, unlabelled compounds (Figure 15A). As expected, the binding of 2 nM [3H]AEA to cytosolic protein(s) was reduced (down to ~10%) by an excess of unlabelled AEA. A less pronounced, yet significant, ~50% displacement was observed using the AEA congener N-arachidonoyldopamine. However, 2-arachidonoylglycerol and N-palmitoylethanolamine could displace only ~15%–20% of the bound [3H]AEA. Finally, arachidonic acid, a catabolic product of AEA, and two different AEA uptake inhibitors, (S)-10-(4-hydroxybenzyl)-oleoylethanolamide (OMDM1) and N-(2-methyl-4-hydroxyphenyl)-arachidonamide (VDM11) (De Petrocellis et al., 2000; Ortar et al., 2003), showed only ~5% displacement of bound [3H]AEA (Figure 15A). These results suggest the presence of AEA binding proteins within the cytosol, which appear to be different from those that are responsible for the transport of AEA across the plasma membrane.

4.10 Gel filtration and [³H]AEA-binding activity

Analysis of the fractions derived from a gel filtration column suggested that [³H]AEA eluted after 17 min (Figure 15B) with an elution profile only partially superimposable to that of the cytosolic proteins, indicating that AEA was primarily associated with specific protein(s) with an apparent molecular weight of 63 ± 25 kDa (Figure 15B and Table 3). Interestingly, the presence of a shoulder in the elution profile (fraction 6) and of a minor peak in fraction 11 suggests that AEA might bind to a variety of cytosolic proteins ranging from < 660 kDa to < 43 kDa. However, we analyzed only the most active fractions (7–9).

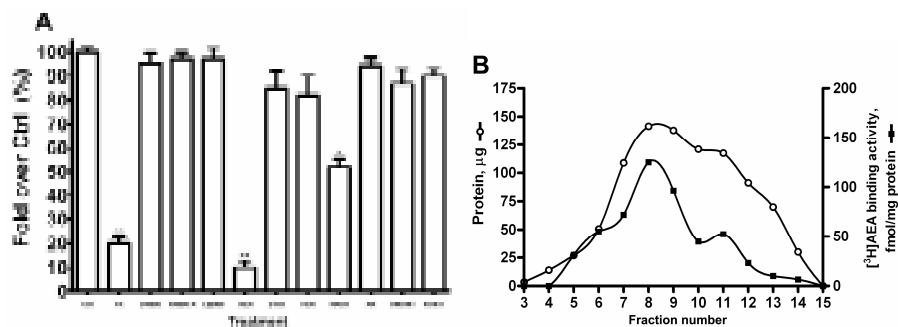


Figure 15. Identification of AEA-binding sites within the cytoplasm. (A) Analysis of the molecular nature and substrate specificity of the [3H]AEA binding sites in the cytosolic fractions of mouse keratinocytes. Cytosolic preparations were incubated with 2 nM [3H]AEA and then incubated with protease K (PK), DNase I (DNase), RNase A, pancreatic lipase C (Lipase), unlabelled AEA, 2-arachidonoylglycerol (2-AG), N-palmitoylethanolamine (PEA), N-arachidonoyldopamine (NADA), arachidonic acid (AA), or two AEA uptake inhibitors, OMDM1 and VDM11. Results are expressed as percentage of untreated cytosol (Ctrl, 100% = 68 ± 5 fmol/mg protein). *p < 0.05 versus Ctrl; **p < 0.01 versus Ctrl. Error bars represent standard error of the mean (SEM) of at least two independent experiments, each performed in triplicate. (B) Partial purification of AEA-binding proteins by gel-filtration chromatography. Cytosolic extracts were eluted on a gel-filtration column (Zorbax GF-450), and the resulting fractions were analyzed for protein content (B) and [3H]AEA-binding activity (-).

Fraction	Total Activity (fmol [3H]AEA)	Protein (µg)	Specific Activity (fmol [3H]AEA/mg)
Cytosol	60.8	0.9	67.5
1	ND ^a	ND	ND
2	ND	ND	ND
3	ND	3.4	ND
4	ND	13.9	ND
5	0.8	26.9	29.7
6	2.8	50.6	55.3
7	7.8	108.9	71.6
8	17.7	141.5	125.1
9	13.3	137.9	96.4
10	5.4	120.9	44.7
11	6.2	117.4	52.8
12	2.1	91.2	23.0
13	0.7	70.0	10.0
14	0.2	30.1	6.6
15	ND	2.0	ND

^aND indicates not detectable

Table 3. Purification of intracellular anandamide-binding sites from skin keratinocytes

4.11 Nano-LC ESI-MS/MS identification of affinity-purified AEA-binding proteins

The most AEA-binding-rich fractions (7–9), amounting to ~65% of the total AEA-binding activity, were pooled, labeled by incubation with 20 μ M b-AEA for 1 hr, and loaded onto a monomeric avidin column for further purification by affinity chromatography. Then these proteins were separated by 2D PAGE (Figure 16). By comparing the 2D PAGE profiles of the affinity-purified samples with a mock-purified control (Figure 16A), we identified several specific spots (Figure 16B). Among these, we focused on three major spots (spot 4, 5, and 6) of apparent molecular mass of ~50–70 kDa. Our analysis did not include low abundance protein spots because of difficulties in obtaining satisfactory protein identification by MS. These spots were excised from the gel for tryptic digestion and the resulting peptides were analyzed by nano-liquid chromatography electrospray ionization tandem mass spectrometry (nano-LC ESI-MS/MS), thanks to an external factory (Proteome Factory AG Berlin, Germany; <http://www.proteomefactory.com>). Peptide masses were searched using Mascot engine with a tolerance of 300 ppm.

The database search resulted in heat shock protein 70.2 (Hsp 70.2) and serum albumin, while the spot 6 led to a protein score too low to be identified. The coordinates (molecular mass and pI) of the detected spots were estimated by interpolation with standard proteins, and were in good agreement with the nominal mass and calculated isoelectric point values of the proteins identified by MS (Figure 16B). Notably, serum albumin has been described to bind AEA in vitro with high affinity (Bojesen and Hansen, 2003; Giuffrida et al., 2000), thus supporting our proteomic analysis. The results of the MS analysis were confirmed by western blotting analysis of the affinity-purified sample, performed using commercially available antibodies against Hsp70 and serum albumin (Figure 16E). Although our MS data point toward Hsp70.2 which is constitutively expressed in the cell cytoplasm in most tissues, including epidermis, it could not be excluded that other members of Hsp70 family, a group of highly related chaperonins that have remarkable sequence identity, might bind AEA probably through their well-conserved binding domains.

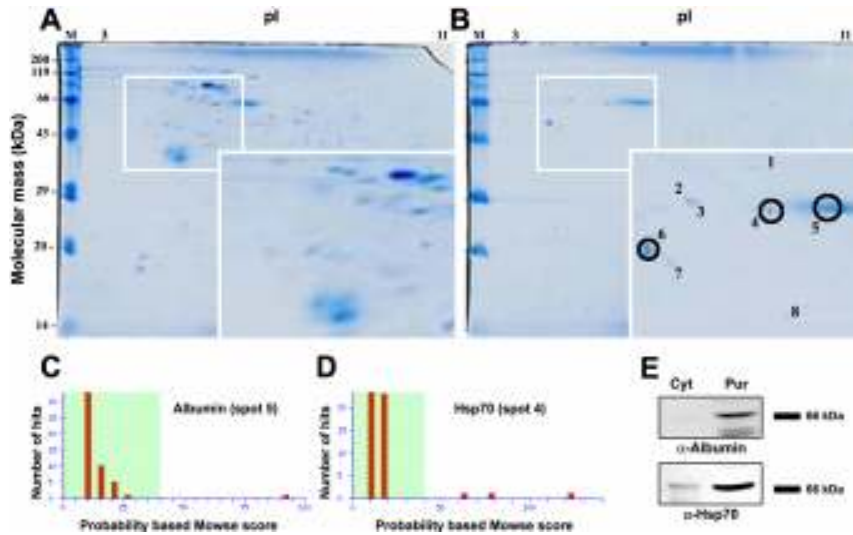


Figure 16. Gel electrophoresis and mass spectrometry identification of the affinity-purified AEA-binding proteins. (A–D) Representative bidimensional electrophoresis (2D-PAGE) gels of mock-purified (A) and affinity-purified (B) samples. Nonspecifically and specifically eluted proteins were resolved by 2D-PAGE on nonlinear pH 3–11 isoelectrofocusing strips, followed by separation on a 12% SDS-PAGE gel in the second dimension. Proteins were visualized by colloidal Coomassie staining. In the insets, high-magnification views of the gels of a selected area are shown. Circled spots indicate proteins further subjected to mass spectrometry. Mascot search results and probability plots corresponding to albumin (C) and Hsp70 (D). (E) Western blotting analysis of cytosol (cyt) and affinity-purified sample (Pur), using antibodies against serum albumin and Hsp70.

4.12 *In vitro* analysis of Hsp70-AEA interaction

In order to confirm the physical interaction between Hsp70.2 and AEA, we developed an *in vitro* method adapted for protein-lipid interaction studies. Hsp70.2 is highly conserved between human and mouse, showing homology with 96% amino acid identity. Human and mouse serum albumin is also very conserved, with over 71% identity. Therefore, these high levels of identity allowed us to shift our study from mouse to human models. We incubated various [3H]AEA concentrations for 1h, AEA binding to human Hsp70 was determined by counting the radioactivity retained by the resin-bound proteins. The procedure was first validated by analyzing AEA affinity for human serum albumin (HSA), because it is known that albumin binds AEA with a Kd value in the nanomolar range at 23 °C (Bojesen and Hansen, 2003; Giuffrida et al., 2000). We found that although the resin *per se* did not retain a significant amount of radioactivity, 15 nmol resin-adsorbed HSA was able to bind [3H]AEA in a concentration-dependent manner, typical of a saturable process (Figure 17A), with apparent Kd and Bmax values of $0.8 \pm 0.1 \mu\text{M}$ and $2.3 \pm 0.2 \text{ nmol/mg}$ of protein, respectively. Next, the assay for the detection of Hsp70-AEA complexes was carried out with 12 nmol resin-bound protein. As shown in Figure 17B, AEA exhibited saturable binding also to Hsp70. The experimental data were fitted and the results obtained were that the hyperbola had an apparent Kd value of $3.7 \pm 0.5 \mu\text{M}$ and a Bmax of $1.9 \pm 0.1 \text{ nmol/mg}$ of protein, indicating that Hsp70 binds AEA with a ~fivefold lower affinity than HSA. These results suggest that there are AEA-binding proteins in the cytosol different from the ones responsible for its transport across the plasma membrane.

4.13 Effect of Hsp70 overexpression on AEA uptake in SH-SY5Y cells

We assessed the effect of Hsp70.2 overexpression on AEA uptake in human neuroblastoma SH-SY5Y cells transiently transfected with the expression vector pcDNA-human Hsp70.2. After 24 hr, expression levels of Hsp70.2 in the cells were assessed by immunofluorescence, using an anti-Hsp70 antibody. We found that the overexpression of Hsp70.2 increased ~5-fold [3H]AEA uptake, from 0.40 ± 0.10 pmol/min per mg of protein in mock-transfected cells to 2.12 ± 0.20 pmol/min per mg of protein in Hsp70.2-transfected (Figure 17C). As a control, the addition of 5 μ M OMDM-1 minimized the transport of AEA across the cell membrane (Figure 3C). Coimmunostaining of exogenous Hsp70.2 and b-AEA showed a marked colocalization of the two molecules (Figures 17D–17F). As indicated in the merged picture (Figure 17F, arrowheads in the inset), an array of b-AEA-positive tubular structures was also positive for Hsp70.2. Moreover, a diffuse cytosolic distribution for both substances was observed. Interestingly, tubular structures with both Hsp70.2 and b-AEA stainings were observed in the close proximity of plasma membrane (Figure 17D–17F, asterisks), suggesting a potential interaction between these two molecules also at the level of the cell membrane.

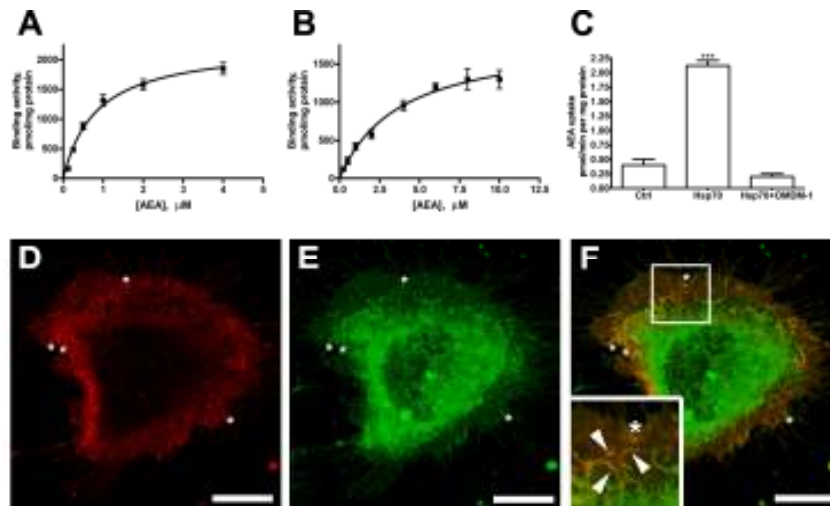


Figure 17. AEA-binding of serum albumin and Hsp70 (A and B) AEA binding to 5 mg albumin (A) or Hsp70 (B) immobilized to 10 ml resin was determined by means of a batch method. The resin-adsorbed proteins were incubated with varying concentrations of AEA for 30 min at 25 °C. Nonspecific adsorption of AEA to cellular membranes or cell supports was estimated by running the identical experiments at 4 °C, and was subtracted from each data point. The lines drawn are the best fit of the data to one-site-binding hyperbola. Values are means \pm SEM of at least two independent experiments, each performed in triplicate. Overexpression of Hsp70.2 in SH-SY5Y cells. (C) Effect of Hsp70.2 overexpression (Hsp70) versus control (Ctrl) on [3H]AEA uptake by SH-SY5Y cells, grown in the absence or in the presence of 5 μ M OMDM1 (Hsp70 + OMDM-1). *** $p < 0.0001$ versus Ctrl. (D–F) Double immunofluorescence of Hsp70.2 (red) and b-AEA (green). The superimposition of the two stainings revealed that Hsp70.2 and b-AEA colocalize in tubular structures within the cytosol (arrowheads in the inset) or near to the plasma membrane (asterisks). The images are representative of three independent experiments, and in each case five fields were examined. Scale bar, 10 μ m.

CHAPTER 5. DISCUSSION

In our studies we report the characterization of a biotinylated derivative of anandamide and show through biochemical, morphological and functional assays that b-AEA is a good tool to visualize this endocannabinoid inside the cells. Moreover we demonstrate that this molecule allowed us to clarify some of the routes through which AEA could be accumulated and transported in the cells.

In the last years all the pathways of biosynthesis and degradation of AEA have been well clarified, leading to the cloning and characterization of the enzyme responsible for AEA degradation FAAH (McKinney and Cravatt, 2005) and the one responsible of its synthesis, NAPE-PLD (Okamoto et al., 2004). To be metabolized by FAAH, AEA must be transported across the plasma membrane to the intracellular compartments where FAAH is localized (Oddi et al., 2005). The mechanism of AEA uptake has remained elusive and to date there is only a general consensus on the fact that AEA movement through the plasma membrane is rapid, saturable, temperature-dependent, and energy (supplied as ATP or ion gradients)-independent (Battista et al., 2005; Glaser et al., 2005; Hillard and Jarrahian, 2005). Many studies described a transporter-mediated uptake of AEA via a selective “anandamide membrane transporter,” while only few papers proposed that the transport occurs by simple diffusion or endocytosis via caveolae/ lipid rafts (Glaser et al., 2005; McFarland et al., 2004a). As a matter of fact, the lack of cloning and expression of the purported transporter protein has prevented the development of molecular tools like oligonucleotides or antibodies, which are able to give definitive proof of the presence of a true transporter on the cell surface. In addition AEA analogs able to visualize AEA movements are still missing. In fact besides radiolabeled AEA, only two other compounds have been created to investigate these aspects of AEA metabolism. The first compound is a fluorescein isothiocyanate-conjugated analog of AEA named SKM 4-45-1 (Muthian et al., 2000). This substance becomes fluorescent upon hydrolysis by cytosolic esterases, releasing the fluorescein moiety. But its use should be restricted to cells that express enough esterase activity (Muthian et al., 2000) and is not suitable to visualize AEA adsorption on the cell surface

(Oddi et al., 2005). The second compound, LY2318912, has been described as a potent, competitive inhibitor of AEA uptake that has made it possible to identify a high-affinity binding site specifically involved in the transport of this endocannabinoid (Moore et al., 2005). However its good employment has been called into question because one of its congeners, LY2183240, is also a potent inhibitor of FAAH (Alexander and Cravatt, 2006; Felder et al., 2006). In this scenario the biotinyl derivative of AEA studied in our work, seems to be a unique tool for the visualization of AEA accumulation by fluorescence microscopy techniques, which are safer, cheaper and easier to use than radiographic methods. We chose to modify the polar head of AEA because previous studies indicated that the kinetics of AEA uptake is sensitive to the modification of the arachidonate moiety, whereas changes in the ethanolamide region are ineffective (Piomelli et al., 1999; Muthian et al., 2000). This molecular properties could also assure a very low affinity for both CB1 and CB2 receptors and almost no activity for TRPV1 receptors and for FAAH (Di Marzo et al., 2004). It seems noteworthy that the biochemical profile of b-AEA shows that it is well recognized only by mechanisms responsible for AEA transport but not by other elements of the endocannabinoid system. Accordingly, the biotin derivative of AEA contains the four *cis* non-conjugated double bond motifs that lead to the U-shaped conformation fundamental for the interaction with the transport machinery (Piomelli et al., 1999). On the other hand, the hydroxyl group of AEA, considered important for the interaction with FAAH (Piomelli et al., 1999), is not available in b-AEA because it is derivatized with the biotin tag. Regarding the possible interaction between b-AEA and CB1R, we found that b-AEA interacts with CB1R moderately and only at micromolar concentrations. Further assays aimed at determining the effect of b-AEA on the binding constants for CP55.940 demonstrated that b-AEA does not affect K_d but reduces B_{max} almost by half. These findings demonstrate that b-AEA does not bind to the ligand binding site of the receptor but rather interferes with CB1R by some other “noncompetitive” mechanism(s). Another important issue concerns the possible role of CB1R on AEA uptake. In fact we found that the blockade of CB1R with SR141716 significantly reduced b-AEA uptake. In keeping with previous studies from our (Oddi et al., 2005; Maccarrone et al., 2000b) and other (Ortega-Gutierrez et al., 2004) laboratories, showing that AEA transport is partly inhibited (by ~20%) by SR141716, this result supports the notion that CB1R is somehow involved in the internalization of AEA and that the cellular uptake of AEA is a complex process that involves

multiple proteins. Together, these observations might open the avenue to new structure-activity relationship studies aimed at elucidating the molecular determinants that confer to b-AEA specificity over AEA itself. In agreement with this, it should be recalled that the transporter-mediated movement across the plasma membrane and the cytosolic trafficking, are key steps in regulating the biological activity of AEA, both centrally and peripherally.

For this reason we decided to investigate through our biotinylated probe, where and how AEA is internalized inside the cells.

Regarding the intracellular sites in which AEA could be stored, we have shown for the first time that, once taken up by the cell AEA is rapidly targeted to lipid bodies. These ubiquitous organelles have been originally described as intracellular stores for neutral lipids and, more recently, they have been linked to transport routes pivotal for lipid trafficking, homeostasis and signalling (Martin and Parton, 2006). By kinetic and subfractionation studies, we also demonstrated that cells with a larger LD compartment display an increased capacity to accumulate and metabolize AEA. Furthermore we demonstrated an overlap between LD compartment and FAAH, which is presumably instrumental for the rapid degradation of AEA stored in these organelles. Taken together, our findings lend biochemical support to an hypothetical model that predicts the existence of a cellular compartment where AEA sequestration can allow its accumulation well beyond the concentration gradient. By functioning as anandamide reservoirs, adiposomes could sequester AEA in a form that is not in free equilibrium with the extracellular pool, thus keeping the intracellular concentration of free AEA very low. Moreover, thanks to their high mobility within the cell (Nan et al., 2006), and to their morpho-functional connection with FAAH, adiposomes can also act as shuttles for the rapid and efficient delivery of AEA from the plasma membrane to the intracellular sites, where hydrolysis takes place.

This function could also be addressed to other components in the cytosol that are able to bind and transport AEA to FAAH or to internal sites of accumulation, like adiposomes. AEA is in fact a lipophilic molecule and its simple, non-ordered diffusion through the aqueous cytoplasm to intracellularly located targets is unlikely to be fast enough to account for the rate and the extent of intracellular accumulation and metabolism of this endocannabinoid (Beltramo et al., 1997; Hillard and Jarrhian, 2000; Jacobsson and Fowler, 2001; Maccarrone et al., 2000b; Ortega-Gutierrez et al., 2004; Rakhshan et al., 2000). From this point of view, an “organized

system'' has been hypothesized for the efficient delivery of AEA to its hydrolase FAAH, and/or to other potential internal targets (Hillard and Jarrahan, 2003). Experimental data suggested the involvement of a lipid rafts/caveolae endocytic pathway for the transmembrane transport of AEA, as well as for its recycling after catabolism (McFarland et al., 2004b). Another possibility is that some soluble proteins ferry AEA through the cytoplasm. We sought to address this issue using our b-AEA and keratinocytes as an experimental model to explore the presence of constitutive intracellular AEA transporters. In preliminary experiments, we found that the cytosolic extracts contained a specific AEA-binding activity associated with proteins and insensitive to OMDM1 and VDM11 suggesting that the cytosolic proteins involved in intracellular AEA binding were different from those that are responsible for the transmembrane transport of AEA. Interestingly, we found that AEA binding was specifically inhibited by N-arachidonoyldopamine (NADA) but not by 2-arachidonoylglycerol, palmitoylethanolamine (PEA), or arachidonic acid, indicating that ligand recognition by the cytosolic AEA carrier(s) implies stringent structural determinants. Next, by using affinity chromatography, we were able to isolate several AEA-interacting proteins in the cytosolic extract from mouse epidermal keratinocytes. Among these, we identified by MS the proteins corresponding to two major spots: serum albumin and Hsp70.2. The identity of these proteins was subsequently confirmed by western blotting and immunofluorescence. Albumin has been demonstrated to bind AEA with high affinity in the extracellular milieu (Bojesen and Hansen, 2003; Giuffrida et al., 2000), but this is the first evidence that endogenous albumin interacts with AEA within the cell acting as an intracellular AEA transporter (AIT). Since the levels of albumin vary within the cytosol of different cell lines, and that this protein is particularly expressed in actively metabolizing or developing tissues, it could be proposed that albumin has a role in controlling the bioavailability of AEA in multiple functional contexts.

Our MS data, together with the experimental molecular mass and pI, identified also Hsp70.2 as an AEA binding protein. which is constitutively expressed in the cell cytoplasm in most tissues, including epidermis. In order to confirm the interaction between Hsp70 and AEA, we developed an *in vitro* batch method. By utilizing pure proteins, we found that Hsp70, alike HSA, was able to bind AEA in a concentration-dependent manner, typical of a saturable process, though with a lower affinity than HSA. We confirmed the intracellular localization of Hsp70.2 by confocal microscopy,

showing that it has a predominant cytoplasmic staining partially overlapped to that of b-AEA. We also observed costaining of Hsp70.2 and b-AEA close to the plasma membrane, suggesting that Hsp70.2 might interact with AEA also at this level.

In conclusion our work report unprecedented evidence that b-AEA is a suitable tool to visualize AEA in the cells. In fact we succeeded in uncovering novel aspects of intracellular distribution of AEA, providing the first evidence for the involvement of adiposomes in AEA accumulation and degradation and for the existence of cytosolic transporters which might form a delivery system active in cytosol, plasma membrane, nucleus, and endoplasmic reticulum, to rapidly and efficiently assist the intracellular trafficking of AEA.

CHAPTER 6. EXPERIMENTAL PROCEDURES

6.1 Materials

Chemicals were of the purest analytical grade. Anandamide, Resiniferatoxin, CP55.940, 1-stearoyl-2-arachidonoyl-sn-glycerol, 2-oleoylglycerol, AEA, HSA, bovine serum albumin, human Hsp70 (cod. H7283) and the anion-exchange resin diethylaminoethyl (DEAE)-Sephacrose were from Sigma Chemical (St. Louis, MO); URB597, VDM11 and OMDM1 were from Alexis Corporation; SR114528 and SR144528 were a kind gift from Sanofi-Aventis Recherche (Montpellier, France). PEA and NADA were from Tocris Cookson (Bristol, UK). Unlabeled N-arachidonoylphosphatidylethanolamine was synthesized from arachidonic acid and phosphatidylethanolamine as reported (Fezza et al., 2005). N-[3H]arachidonoylphosphatidylethanolamine (200 Ci/mmol), 2-oleoyl[3H]glycerol (20 Ci/mmol), AEA-ethanolamine-1-[3H] (60 Ci/mmol) and 1-stearoyl-2-arachidonoyl[1-14C]-sn-glycerol (55 mCi/mmol) were from ARC; [3H]CP55.940 (163 Ci/mmol), [Arachidonoyl-5,6,8,9,11,12,14,15-3H]AEA (205 Ci/mmol), [3H]oleic acid (60 Ci/mmol), [3H]arachidonic acid (AA) (99 Ci/mmol) and [3H]RTX (43 Ci/mmol) were from Perkin Elmer Life Sciences. YM-10 Centricon devices were purchased from Millipore Co. (Rome, Italy). Rabbit anti-Hsp70 and anti-albumin polyclonal antibodies were obtained from Santa Cruz Biotechnology (Santa Cruz, CA). Mouse anti-biotin monoclonal antibody, goat Alexa Fluor-conjugated secondary antibody, and Prolong anti-fade kit were purchased from Molecular Probes (Eugene, OR). The plasmid expressing human Hsp70.2 (pcDNA3-Hsp70.2) was a kind gift of Dr. Antonio Rossi of the Institute of Neurobiology and Molecular Medicine (National Research Council, Rome, Italy). LipofectAMINE 2000 was from Invitrogen Life Technologies. Culture media, sera, and supplements were obtained from PromoCell (Heidelberg, Germany). Nonyl acridine orange, mouse anti-biotin antibody, goat Alexa Fluor-conjugated secondary antibodies, Image-iTMM FX signal enhancer and Prolong antifade kit were purchased from Molecular Probes (Eugene, OR).

6.2 Cell culture and treatments

HaCaT and SH-SY5Y were maintained in DMEM or RPMI supplemented with 10% fetal bovine serum and cultured as described (Canals et al., 2005; Oddi et al., 2005). To increase triacylglycerol synthesis and storage in the cells, 100 mM oleic acid complexed to albumin was added to the medium, and cells were incubated overnight at 37°C in a 5%CO₂ humidified atmosphere.

6.3 Biochemical analyses

6.3.1 FAAH assay

The assay of FAAH (E.C.3.5.1.4) activity was performed by measuring the release of [3H]EA from [3H-ethanolamine]AEA. (Mor et al., 2004). Mouse brain homogenate (40 µg/test) was incubated with ST compounds for 20 min and then the reaction was initiated by the addition of [3H]AEA, at a final concentration of 10 µM, for 15 min at 37°C in a final volume of 500 µl of 50 mM Tris-HCl (pH 9.0). The reaction was stopped by the addition of 800 µl ice-cold methanol/chloroform (2:1, v/v) with vortexing. The mixture was centrifuged at 3000xg for 5 min, the upper aqueous layer was isolated, put in a vial containing liquid scintillation cocktail and analyzed in a β-counter. FAAH specific activity was expressed as pmol [3H]EA released/min per mg of protein.

6.3.2 NAPE-PLD assay

The NAPE-PLD (E.C. 3.1.4.4) assay was performed as follows (Fezza et al., 2005). Briefly, mouse brain homogenate (200 µg/test) was incubated with ST compounds for 20 min. After, the mixture was incubated with [3H]NArPE (100 µM) for 30 min at 37°C in 200 µl of 50 mM Tris-HCl (pH 7.4) containing 0.1% Triton X-100. A mixture of chloroform/methanol (2:1, v/v, 600 µl) was added to stop the reaction. Then the samples were vortexed and centrifuged at room temperature, and the lower organic phase was dried. The pellet was resuspended in 20 µl of methanol and was subjected to RP-HPLC analysis. Specific activity of NAPE-PLD was expressed as pmol of [3H]AEA released from [3H]NArPE per min per mg of protein.

6.3.3 AMT assay

The activity of AEA uptake was studied in intact HaCaT cells (Maccarrone et al., 2008). Cells were incubated for 10 min at 37°C with [3H]AEA or [3H]b-AEA as substrate and washed three times in 1 ml of PBS containing 1% BSA; then, they were resuspended in 0.5 ml (0.5 M) of NaOH and measured in a scintillation counter. To further discern non-carrier-mediated from carrier-mediated transport of [3H]AEA or [3H]b-AEA across cell membranes, control experiments were carried out at 4°C. The effect of different compounds on [3H]AEA or [3H]b-AEA uptake was determined by adding each substance directly to the incubation medium at the indicated concentrations (Maccarrone et al., 2003a).

6.3.4 DAGL assay

The synthesis of 2-AG made by DAGL (E.C.3.1.1.4) was evaluated as follows (Maccarrone et al., 2008). Briefly, mouse brain homogenate in Tris HCl 50 mM (pH 7.4) were centrifuged at 4°C at 800xg (5 min) and the supernatants at 10,000xg (25 min). The membranes obtained at 10,000xg (200 µg/test) were at first incubated with ST compound for 20 min in 50 mM Tris-HCl with 1 mM CaCl₂ (pH 7.4) and then with DAG (500 µM) for 15 min at 37°C. After the incubation, a mixture of chloroform/methanol (2:1, v/v) was added to stop the reaction, and the organic phase was dried and fractionated by thin layer chromatography (TLC) on silica, using polypropylene plates with chloroform/methanol/NH₄OH (95:5:0.3, v/v/v) as eluent. The release of [14C]-2-AG was measured by cutting the corresponding TLC bands, followed by scintillation counting.

6.3.5 MAGL assay

MAGL (E.C. 3.1.1.23) activity was evaluated as reported (Maccarrone et al., 2008). The supernatant proteins (100 µg/test) of mouse brain obtained at 10000xg were incubated for 20 min with the ST compound in Tris HCl 50 mM (pH 7.5) and then with 2-oleoyl-[3H]glycerol (10 µM) for 30 min at 37 °C. The reaction was stopped with chloroform/methanol (2:1, v/v). The mixture was centrifuged at 3000xg for 5 min, the upper aqueous layer containing [3H]glycerol was prelevated and counted in a β-counter.

6.3.6 Receptor binding assay

Membrane fractions isolated from mouse brain (for CB1R and TRPV1 binding) and from mouse spleen (for CB2R binding) were obtained as described (Maccarrone et al., 2008). These membrane fractions (100 µg/test) were at first incubated with the ST compound for 20 min, then with 400 pM [³H]CP 55,940 (for CB1R and CB2R binding) or with 500 pM [³H]RTX (for TRPV1 binding), for 1h at 30°C and used in rapid filtration assay as described³. Unspecific binding was determined in the presence of an excess (1 µM) of cold CP 55,940 (for CB1R and CB2R binding) or RTX (for TRPV1 binding). The filters were washed two times with a cold buffer (Tris HCl 50 mM, 1mg/mL BSA, pH 7.4) and put in a vial containing scintillation cocktail liquid. After 6 hours the vials were counted with a β-counter.

6.4 Synthesis of b-AEA

We prepared b-AEA using the EZ-Link Biotin-PEOAmine. Briefly, the AA was activated using an amide-coupling reagent and then treated with the biotin tag in basic medium (Maccarrone et al., 2006, WO20071). The synthesis of the radiolabeled [³H]b-AEA was carried out under the same experimental conditions using a mix of AA and [³H]AA (specific activity, 10 mCi/mmol).

6.5 Western blot analyses

Western blotting was performed according to standard procedures (Maccarrone et al., 2003a). The following antibodies were used to immunodetect specific markers of different subcellular compartments: anti-actin (cytosol), anti-ER (endoplasmic reticulum), anti-caveolin-1 (caveolae), anti-Na⁺/K⁺- ATPase (plasma membrane), and anti-adipophilin (lipid droplets). Serum albumin and Hsp70 were immunodetected using antibodies that are validated for detection of these proteins of both human and mouse origin. All the antibodies were purchased from Santa Cruz Biotechnology, Inc. (Santa Cruz, CA).

6.6 Subcellular fractionation of [³H]AEA-treated cells

HaCaT cells were grown overnight in the presence of 100 mM oleic acid; they were then collected with trypsin, washed twice with Ca²⁺/Mg²⁺-free HBSS, and resuspended in DMEM supplemented with 0.5% fetal bovine serum. Subsequently, cells were preincubated for 10 min with 100 nM URB597 to inhibit FAAH activity. [³H]AEA or [³H]oleic acid (2 mCi/108 cells), or nonyl acridine orange (10 mM) was added to the cells and maintained for 15 min under continuous agitation. Lipid bodies were isolated essentially as described (Yu et al., 2000). Briefly, cells were washed twice with Ca²⁺/Mg²⁺-free HBSS and resuspended in 3 mL of disruption buffer (25 mM Tris-HCl, 100 mM potassium chloride, 1 mM EDTA, and 5 mM EGTA, pH 7.4, supplemented with 10 mg/mL leupeptin, 0.7 mg/mL pepstatin A, and 0.1 mM phenylmethylsulfonyl fluoride). Cells were disrupted by dounce homogenizer and mixed with an equal volume of disruption buffer containing 1.08 M sucrose. After centrifugation at 1500 g for 10 min to spin down nuclei, the supernatant was transferred to a 12-mL ultracentrifugation tube, and was overlaid sequentially with 2.0 mL each of 0.27 M sucrose buffer, 0.13 M sucrose buffer, and Top solution (25 mM Tris-HCl, 1 mM EDTA, and 1 mM EGTA, pH 7.4), followed by centrifugation at 150 500 g for 2 h. Eight fractions of 1.5 mL were collected from top to bottom: the buoyant lipid bodies (1 and 2), the mid-zone between lipid bodies and cytosol (3 and 4), and the cytosol (5–8). The microsomal pellet and nuclei (pt) were washed and resuspended in 1.5 mL Top solution by sonication. Aliquots of all nine fractions were used for the analysis of protein content, radioactivity or fluorescence ($\lambda_{ex} = 450$ nm; $\lambda_{em} = 640$ nm). To determine tritium content, 100 μ L of each fraction was added to individual scintillation vials containing 3.5 mL UltimaGold XR (Perkin-Elmer; Boston, MA), and tritium was quantified in a Beckman LS 6000IC scintillation counter (Fullerton, CA). To analyze the amount of intact [³H]AEA, the fractions were extracted with a mixture of chloroform: methanol (2:1, v/v), the organic phase was dried and the pellet was subjected to RP-HPLC analysis on a Nelson 1022 Plus Chromatograph (Perkin Elmer). The separation of [³H]AEA and [³H]AA was carried out on a C18 (5 μ m x 3.0 mm x 150 mm) column (Waters; Milford, MA), with a mobile phase of methanol: water:acetic acid (85:15:0.1, v/v/v) at a flow rate of 0.8 mL/min (Maccarrone et al., 1999). The identity of radiolabeled [³H]AEA and [³H]AA was confirmed by monitoring through UV detection the separation

of authentic cold standards, and radioactivity was quantified by a TRICARB 2100TR counter (Perkin-Elmer).

6.7 Extraction of cytosolic proteins

To isolate cytosolic proteins, epidermal mouse keratinocytes were explanted from the skin of newborn mice. To this end, 25 newborn mice (1–2 days old) were killed by cervical dislocation after anesthesia and the skin was removed, rinsed in Ca²⁺/Mg²⁺-free PBS, and incubated in 1% trypsin in PBS for 18 hr at 4°C. Explanted skins were transferred to PBS at RT and aspirated with a Pasteur pipette to loosen the epidermis, which was subsequently removed, using forceps and a tungsten needle, and extensively washed with ice-cold PBS. The cell extracts were resuspended in hypotonic buffer (5 mM Tris-HCl [pH 7.4], 10mMKCl, 5mMEDTA, 1mM4-[2 aminoethyl]benzenesulfonyl fluoride, and 1 mM DTT) and lysed on ice using a loose-fitting Dounce homogenizer. After low-speed centrifugation to remove nuclei and intact cells, the cytosolic fraction was prepared by centrifuging supernatants at 250,000 x g for 2 hr at 4°C. The cytosol samples were dialyzed against PBS for 5 hr at 4°C, and the protein concentration was measured by the Bradford assay kit (Bio-Rad, Hercules, CA).

6.8 Fractionation by gel filtration

Size-exclusion high-performance liquid chromatography measurements were performed on a PE Series 200 System (Perkin-Elmer) using a Zorbax GF-450 gel-filtration column (Agilent Technologies, Santa Clara, CA) that allows separation within a range from 10 to 1000 kDa. Cytosol (150 ml) was incubated with 2 nM [3H]AEA and fractionated on the Zorbax GF-450 column using PBS as eluent, at RT and a flux rate of 1 ml/min. Protein concentration and radioactivity of the collected fractions were monitored using an ultraviolet-visible detector and a radiodetector, respectively. Protein size was determined by comparison with the following gel-filtration grade molecular mass standards (GE Healthcare, Sweden): ovalbumin (43 kDa), albumin (67 kDa), aldolase (158 kDa), and thyroglobulin (669 kDa).

6.9 Biotin-affinity chromatography

The cytosolic fraction was preliminarily cleared of endogenous biotinylated proteins by passing through a monomeric avidin column (Pierce, Rockford, IL), equilibrated in PBS. The cleared extract was mixed with 20 mM b-AEA, incubated for 30 min at RT, and applied to freshly prepared monomeric avidin column. After sample application, the avidin column was washed extensively with PBS, until the absorbance value at 280 nm reached the baseline. Then, bound proteins were competitively eluted with PBS containing 2 mM biotin, and were concentrated on YM-10 Centricon filters for further analysis. Nonspecific elution from the affinity column was identified by collecting the eluate from the column loaded with cleared cytosol, but without added b-AEA.

6.10 Nano-LC ESI-MS/MS

Protein identification using nano-LC ESI-MS/MS was conducted by the Proteome Factory (Proteome Factory AG Berlin, Germany; <http://www.proteomefactory.com>). The MS system consists of an Agilent 1100 NanoLC system (Agilent, Germany), PicoTip emitter (New Objective, USA), and an Esquire 3000 plus ion trap MS (Bruker, Bremen, Germany).

6.11 [³H]AEA-binding assay by DEAE

For AEA-binding studies with HSA and Hsp70, a variant of the conventional pull-down assay was used. This method exploits the ability of DEAE resin to bind proteins but not free lipids. Purified and delipidated proteins (5 mg, corresponding to 15 nmol and 12 nmol HSA and Hsp70, respectively) were adsorbed to 30 ml slurry DEAE sepharose (50%, v/v) by incubating the suspension in 20 mM Tris-HCl (pH 7) for 15 min at RT. Then, DEAE-adsorbed proteins were incubated with various concentrations of [³H]AEA for 1 hr at RT, and the suspension was vortexed every 10 min. The final volume was 200 ml, and the total concentration of methanol did not exceed 1%. At the end of the incubation, 1 ml ice-cold 20 mM Tris-HCl was added to stop the reaction, and the resin was collected by centrifuging at 7000xg for 5 min, and washed twice in the same way. Then, DEAE was resuspended in 500 ml 20 mM Tris-HCl and added to a vial containing

scintillation liquid, and radioactivity was measured in a beta-counter analyzer. Each value was determined in triplicate and was corrected against a blank (no protein added) assayed in parallel. The counts of blanks were never more than 7% of the total amount of ligand added. Binding data for HSA and Hsp70 were elaborated through nonlinear regression analysis, using the Prism 4 program (GraphPad Software Inc., San Diego, CA), in order to calculate apparent dissociation constant (Kd) and maximum binding (Bmax) of [3H]AEA.

6.12 Fluorescence microscopy studies

HaCaT cells were plated on collagen-coated glass coverslips. At 24 h after plating, cultures were treated either with 5 mM biotin-tag, as negative control, or with 5 mM b-AEA for 10 min at 37°C in a 5% CO₂ humidified atmosphere. After each treatment, cells were extensively washed, fixed with 4% paraformaldehyde for 30 min at room temperature, and then permeabilized with 0.1% Triton X-100 in PBS for 2 min at 4°C. After a blocking step in Image-iTTM FX signal enhancer for 30 min, cells were incubated for 1 h with anti-biotin primary antibody, diluted 1:100 in Image-iTTM FX signal enhancer. Staining of FAAH was performed using anti-FAAH diluted 1:200. Secondary antibodies conjugated to Alexa Fluor 488 or Alexa Fluor 568 were diluted 1:200 in blocking solution, and were incubated with the specimens for 30 min at room temperature. After washing, the coverslips were mounted using the antifade prolong Gold reagent, and were visualized by Nikon Eclipse E800 fluorescence microscopy (Nikon Instruments, Tokyo, Japan). To visualize lipid droplets, 100 ng/mL Nile Red dye was added to the medium 15 min before fixation, and then during incubation with antibodies.

6.13 Statistical analysis

Data reported in this paper are the means \pm SD of at least three independent experiments, each performed in duplicate. Statistical analysis was performed by the nonparametric Mann-Whitney U test, elaborating experimental data by means of the InStat 3 program (GraphPAD Software for Science, San Diego, CA).

REFERENCES

REFERENCES

Alexander JP, Cravatt BF. The putative endocannabinoid transport blocker LY2183240 is a potent inhibitor of FAAH and several other brain serine hydrolases. *J Am Chem Soc.* 2006. 128:9699–9704.

Al-Hayani A, Wease KN, Ross RA, Pertwee RG, Davies SN. The endogenous cannabinoid anandamide activates vanilloid receptors in the rat hippocampal slice. *Neuropharmacology.* 2001. 41:1000-1005.

Baker D, Pryce G, Davies WL, Hiley CR. In silico patent searching reveals a new cannabinoid receptor. *Trends Pharmacol Sci.* 2006. 1:1-4.

Basavarajappa BS, Yalamanchili R, Cravatt BF, Cooper TB, Hungund BL. Increased ethanol consumption and preference and decreased ethanol sensitivity in female FAAH knockout mice. *Neuropharmacology.* 2006. 50:834-844.

Basavarajappa BS, Yalamanchili R, Cooper TB, Hungund BL. The endocannabinoid system. *Handbook of Neurochemistry and Molecular Neurobiology.* 2008. Vizi, E. Sylvester; Lajtha, Abel (Eds.).

Battista N, Gasperi V, Fezza F, Maccarrone M. The anandamide membrane transporter and the therapeutic implications of its inhibition. *Therapy.* 2005. 2:141–150.

Beltramo M, Stella N, Calignano A, Lin SY, Makriyannis A, Piomelli D. Functional role of high-affinity anandamide transport, as revealed by selective inhibition. *Science.* 1997. 277:1094–1097.

Beltramo M, Piomelli D. Carrier-mediated transport and enzymatic hydrolysis of the endogenous cannabinoid 2-arachidonylethanolamide. *Neuroreport.* 2000. 11:1231-1235.

Berdyshev EV, Schmid PC, Krebsbach RJ, Schmid HH. Activation of PAF receptors results in enhanced synthesis of 2-arachidonoylglycerol (2-AG) in immune cells. *FASEB J.* 2001. 15:2171-2178.

Bisogno T, Sepe N, Melck D, Maurelli S, De Petrocellis L, Di Marzo V. Biosynthesis, release and degradation of the novel endogenous cannabimimetic metabolite 2-arachidonoylglycerol in mouse neuroblastoma cells. *Biochem J.* 1997. 322:671-677.

Bisogno T, Melck D, De Petrocellis L, Di Marzo V. Phosphatidic acid as the biosynthetic precursor of the endocannabinoid 2-arachidonoylglycerol in intact mouse neuroblastoma cells stimulated with ionomycin. *J Neurochem.* 1999. 72:2113-2119.

Bisogno T, Melck D, Bobrov MYu, Gretskaya NM, Bezuglov VV, De Petrocellis L, Di Marzo V. N-acyl-dopamines: novel synthetic CB(1) cannabinoid-receptor ligands and inhibitors of anandamide inactivation with cannabimimetic activity in vitro and in vivo. *Biochem J.* 2000. 351:817-824.

Bisogno T, Maccarrone M, De Petrocellis L, Jarrahian A, Finazzi-Agrò A, Hillard C, Di Marzo V. The uptake by cells of 2-arachidonoylglycerol, an endogenous agonist of cannabinoid receptors. *Eur J Biochem.* 2001. 268:1982-1989.

Bisogno T, Howell F, Williams G, Minassi A, Cascio MG, Ligresti A, Matias I, Schiano-Moriello A, Paul P, Williams EJ, Gangadharan U, Hobbs C, Di Marzo V, Doherty P. Cloning of the first sn1-DAG lipases points to the spatial and temporal regulation of endocannabinoid signaling in the brain. *J Cell Biol.* 2003. 163:463-468.

Bojesen IN, Hansen HS. Binding of anandamide to bovine serum albumin. *J Lipid Res.* 2003. 44:1790-1794.

Bouaboula M, Poinot-Chazel C, Bourrie B, Canat X, Calandra B, Rinaldi-Carmona M, Le Fur G, Casellas P. Activation of mitogen activated protein kinases by stimulation of the central cannabinoid receptor CB1. *Bio J.* 1995. 312:637-641.

Bouaboula M, Hilaiet S, Marchand J, Fajas L, Le Fur G, Casellas P. Anandamide induced PPARgamma transcriptional activation and 3T3-L1 preadipocyte differentiation. *Eur J Pharmacol.* 2005. 517:174-181.

Bracey MH, Hanson MA, Masuda KR, Stevens RC, Cravatt BF. Structural adaptations in a membrane enzyme that terminates endocannabinoid signaling. *Science.* 2002. 298:1793–1796.

Breivogel CS, Griffin G, Di Marzo V, Martin R. Evidence for a new G-protein-coupled cannabinoid receptor in mouse brain. *Mol Pharm.* 2001. 60:155-163.

Burstein SH, Rossetti RG, Yagen B, Zurier RB. Oxidative metabolism of anandamide. *Prostaglandins Other Lipid Mediat.* 2000. 61:29-41.

Cadas H, di Tomaso E, Piomelli D. Occurrence and biosynthesis of endogenous cannabinoid precursor, N-arachidonoyl phosphatidylethanolamine, in rat brain. *J Neurosci.* 1997. 17:1226–1242.

Canals M, Angulo E, Casado V, Canela EI, Mallol J, Vinals F, Staines W, Tinner B, Hillion J, Agnati L, Fuxe K, Ferre S, Lluís C, Franco R. Molecular mechanisms involved in the adenosine A and A receptor-induced neuronal differentiation in neuroblastoma cells and striatal primary cultures. *J. Neurochem.* 2005. 92:337–348.

Cermelli S, Guo Y, Gross SP, Welte MA. The lipid-droplet proteome reveals that droplets are a protein storage depot. *Curr Biol.* 2006. 16:1783–1795.

Cravatt BF, Giang DK, Mayfield SP, Boger DL, Lerner RA, Gilula NB. Molecular characterization of an enzyme that degrades neuromodulatory fatty-acid amides. *Nature.* 1996. 384:83–87.

Cravatt BF, Lichtman AH. The enzymatic inactivation of the fatty acid amide class of signaling lipids. *Chem Phys Lipids.* 2002. 121:135-148.

Dainese E, Oddi S, Bari M, Maccarrone M. Modulation of the endocannabinoid system by lipid rafts. *Curr Med Chem.* 2007. 14:2702–2715.

De Petrocellis L, Bisogno T, Davis JB, Pertwee RG, Di Marzo V. Overlap between the ligand recognition properties of the anandamide transporter and the VR1 vanilloid receptor: inhibitors of anandamide uptake with negligible capsaicin-like activity. *FEBS Lett.* 2000. 483:52–56.

De Petrocellis L, Bisogno T, Maccarrone M, Davis JB, Finazzi-Agrò A, and Di Marzo V. The activity of anandamide at vanilloid VR1 receptors requires facilitated transport across the cell membrane and is limited by intracellular metabolism. *J Biol Chem.* 2001. 276:12856-12863.

Devane WA, Dysarz FA, Johnson MR, Melvin LS, Howlett AC. Determination and characterization of a cannabinoid receptor in rat brain. *Mol Pharmacol.* 1988. 34:605–613.

Devane WA, Hanus L, Breuer A, Pertwee RG, Stevenson LA, Griffin G, Gibson D, Mandelbaum A, Etinger A, Mechoulam R. Isolation and structure of a brain constituent that binds to the cannabinoid receptor. *Science.* 1992. 258:1946–1949.

Di Marzo V, Fontana A, Cadas H, Schinelli S, Cimino G, Schwartz JC, Piomelli D. Formation and inactivation of endogenous cannabinoid anandamide in central neurons. *Nature.* 1994. 372:686–691.

Di Marzo V, De Petrocellis L, Sugiura T, Waku K. Potential biosynthetic connections between the two cannabimimetic eicosanoids, anandamide and 2-arachidonoyl-glycerol, in mouse neuroblastoma cells. *Biochem Biophys Res Commun.* 1996a. 227:281–288.

Di Marzo V, De Petrocellis L, Sepe N, Buono A. Biosynthesis of anandamide and related acylethanolamides in mouse J774 macrophages and N18 neuroblastoma cells. *Biochem J.* 1996b. 316:977–984.

Di Marzo V, Deutsch DG. Biochemistry of the endogenous ligands of cannabinoid receptors. *Neurobiol Dis.* 1998. 5:386-404.

Di Marzo V, Bisogno T, De Petrocellis L, Melck D, Orlando P, Wagner JA, Biosynthesis and inactivation of the endocannabinoid 2-arachidonoylglycerol in circulating and tumoral macrophages. *Eur J Biochem.* 1999. 264:258-267.

Di Marzo V, De Petrocellis, Fezza F, Ligresti A, Bisogno T. Anandamide receptors. *Prostaglandins Leukot. Essent. Fatty Acids*. 2002. 66:377-391.

Di Marzo V, Ligresti A, Morera E, Nalli M, Ortar G. The anandamide membrane transporter. Structure-activity relationships of anandamide and oleoylethanolamine analogs with phenyl rings in the polar head group region. *Bioorg Med Chem*. 2004. 12:5161–5169.

Di Marzo V. The endocannabinoid system: its general strategy of action, tools for its pharmacological manipulation and potential therapeutic exploitation. *Pharmacol Res*. 2009. 60:77-84.

Dinh TP, Carpenter D, Leslie FM, Freund TF, Katona I, Sensi SL, Kathuria S, Piomelli D. Brain monoglyceride lipase participating in endocannabinoid inactivation. *Proc Natl Acad Sci USA*. 2002. 99:10819–10824.

Egertova M, Cravatt BF, Elphick MR. Comparative analysis of fatty acid amide hydrolase and cb(1) cannabinoid receptor expression in the mouse brain: evidence of a widespread role for fatty acid amide hydrolase in regulation of endocannabinoid signaling. *Neuroscience*. 2003. 119:481–496.

Fegley D, Kathuria S, Mercier R, Li C, Goutopoulos A, Makriyannis A, Piomelli D. Anandamide transport is independent of fatty-acid amide hydrolase activity and is blocked by the hydrolysis-resistant inhibitor AM1172. *Proc Natl Acad Sci USA*. 2004. 101:8756–8761.

Felder CC, Joyce KE, Briley EM, Mansouri J, Mackie K, Blond O, Lai Y, Ma AL, Mitchell RL. Comparison of the pharmacology and signal transduction of the human cannabinoid CB1 and CB2 receptors. *Mol Pharmacol*. 1995. 48:443-450.

Felder CC, Dickason-Chesterfield AK, Moore SA. Cannabinoids biology: the search for new therapeutic targets. *Mol Interv*. 2006. 6:149–161.

Fezza F, Gasperi V, Mazzei C, Maccarrone M. Radiochromatographic assay of N-acyl-phosphatidylethanolamine-specific phospholipase D (NAPE-PLD) activity. *Anal Biochem.* 2005. 339:113–120.

Fowler CJ, Ghafouri N. Does the hydrolysis of 2-arachidonoylglycerol regulate its cellular uptake? *Pharmacol Res.* 2008. 58:72–76.

Franklin A, Stella N. Arachidonoylcyclopropylamide increases microglial cell migration through cannabinoid CB2 and abnormal-cannabidiol-sensitive receptors. *Eur J Pharmacol.* 2003. 474:195-198.

Galiègue S, Mary S, Marchand J, Dussosoy D, Carrière D, Carayon P, Bouaboula M, Shire D, Le Fur G, Casellas P. Expression of central and peripheral cannabinoid receptors in human immune tissues and leukocyte subpopulations. *Eur J Biochem.* 1995. 232:54-61.

Gaoni Y, Mechoulam R. Isolation, structure and partial synthesis of an active constituent of hashish. *J Am Chem Soc.* 1964. 86:1646–1647.

Giuffrida A, Rodriguez de Fonseca F, Piomelli D. Quantification of bioactive acylethanolamides in rat plasma by electrospray mass spectrometry. *Anal Biochem.* 2000. 280:87–93.

Glaser ST, Abumrad NA, Fatade F, Kaczocha M, Studholme KM, Deutsch DG. Evidence against the presence of an Anandamide transporter. *Proc Natl Acad Sci USA.* 2003.100:4269–4274.

Glaser ST, Kaczocha M., Deutsch DG. Anandamide transport: a critical review. *Life Sci.* 2005. 77:1584–1604.

Glass M, Dragunow M, Faull RLM. Cannabinoid receptors in the human brain: a detailed anatomical and quantitative autoradiographic study in the fetal, neonatal and adult human brain. *Neuroscience.* 1997. 77:299– 318.

Gocze PM, Freeman DA. Factors underlying the variability of lipid droplet fluorescence in MA-10Leydig tumor cells. *Cytometry.* 1994. 17:151–158.

Goparaju SK, Ueda N, Taniguchi K, Yamamoto S. Enzymes of porcine brain hydrolyzing 2-arachidonoylglycerol, an endogenous ligand of cannabinoid receptors. *Biochem Pharmacol.* 1999. 57:417-423.

Guesdon JL, Ternynck T, Avrameas S. The use of avidin-biotin interaction in immunoenzymatic techniques. *J Histochem Cytochem.* 1979. 27:1131-1139.

Gulyas AI, Cravatt BF, Bracey MH, Dinh TP, Piomelli D, Boscia F, Freund TF. Segregation of two endocannabinoid-hydrolyzing enzymes into preand postsynaptic compartments in the rat hippocampus, cerebellum and amygdala. *Eur J Neurosci.* 2004. 20:441-458.

Guzman M. Cannabinoids: potential anticancer agents. *Nature Rev Cancer.* 2003. 3:745-755.

Hajos N, Kathuria S, Dinh T, Piomelli D, Freund TF. Endocannabinoid transport tightly controls 2-arachidonoyl glycerol actions in the hippocampus: effects of low temperature and the transport inhibitor AM404. *Eur J Neurosci.* 2004. 19:2991-2996.

Hanus L, Abu-Lafi S, Fride E, Breuer A, Vogel Z, Shalev DE, Kustanovich I, Mechoulam R. 2-Arachidonyl glyceryl ether, an endogenous agonist of the cannabinoid CB1 receptor. *Proc Natl Acad Sci USA.* 2001. 98:3662–3665.

Heimann AS, Gomes I, Dale CS, Pagano RL, Gupta A, de Souza LL, Luchessi AD, Castro LM, Giorgi R, Rioli V, Ferro ES, Devi LA. Hemopressin is an inverse agonist of CB1 cannabinoid receptors. *Proc Natl Acad Sci USA.* 2007. 104:20588–20593.

Hillard CJ, Wilkison DM, Edgemond WS, Campbell WB. Characterization of the kinetics and distribution of N-arachidonylethanolamine (anandamide) hydrolysis by rat brain. *Biochim Biophys Acta.* 1995. 1257:249–256.

Hillard CJ, Edgemond WS, Jarrahian A, Campbell WB. Accumulation of N-arachidonylethanolamine (anandamide) into cerebellar granule cells occurs via facilitated diffusion. *J Neurochem.* 1997. 69:631–638.

Hillard CJ, Jarrahian A. The movement of N-arachidonylethanolamine (anandamide) across cellular membranes. *Chem Phys Lipids*. 2000. 108:123–134.

Hillard C, Jarrahian A. Cellular accumulation of anandamide: consensus and controversy. *Br J Pharmacol*. 2003. 140:802–808.

Hillard CJ, Jarrahian A. Accumulation of anandamide: evidence for cellular diversity. *Neuropharmacology*. 2005. 48:1072–1078.

Ho SY, Delgado L, Storch J. Monoacylglycerol metabolism in human intestinal Caco-2 cells: evidence for metabolic compartmentation and hydrolysis. *J Biol Chem*. 2002. 277:1816-1823.

Howlett AC, Fleming RM. Cannabinoid inhibition of adenylate cyclase. Pharmacology of the response in neuroblastoma cell membranes. *Mol Pharmacol*. 1984. 26:532-528.

Howlett AC, Qualy JM, Khachatrain LL. Involvement of Gi in the inhibition of adenylate cyclase by cannabinoid drugs. *Mol Pharmacol*. 1986. 29:307–313.

Howlett AC, Mukhopadhyay S. Cellular signal transduction by anandamide and 2-arachidonoylglycerol. *Chem Phys Lipids* 2000. 108:53-70.

Howlett AC, Barth F, Bonner TI, Cabral G, Casellas P, Devane WA, Felder CC, Herkenham M, Mackie K, Martin BR, Mechoulam R, Pertwee RG. International Union of Pharmacology. XXVII. Classification of cannabinoid receptors. *Pharmacol Rev*. 2002. 54:161-202.

Huang SM, Bisogno T, Trevisani M, Al-Hayani A, De Petrocellis L, Fezza F, Tognetto M, Petros TJ, Krey JF, Chu CJ, Miller JD, Davies SN, Geppetti P, Walker JM, Di Marzo V. An endogenous capsaicin-like substance with high potency at recombinant and native vanilloid VR1 receptors. *Proc Natl Acad Sci USA*. 2002. 99:8400–8405.

Jacobsson SO, Fowler CJ. Characterization of palmitoylethanolamide transport in mouse Neuro-2a neuroblastoma and rat RBL-2H3 basophilic leukaemia cells: comparison with anandamide. *Br J Pharmacol*. 2001. 132:1743–1754.

James G, Butt AM. P2Y and P2X purinoceptor mediated Ca²⁺ signalling in glial cell pathology in the central nervous system. *Eur J Pharmacol.* 2002. 447:247-260.

Jordt SE, Julius D. Molecular basis for species-specific sensitivity to "hot" chili peppers. *Cell.* 2002. 108:421-430.

Jung, J, Hwang SW, Kwak J, Lee SY, Kang, CJ, Kim WB, Kim D, Oh U. Capsaicin binds to the intracellular domain of the capsaicin-activated ion channel. *J Neurosci.* 1999. 19:529-538.

Karlsson M, Contreras JA, Hellman U, Tornqvist H, Holm C. cDNA cloning, tissue distribution, and identification of the catalytic triad of monoglyceride lipase. Evolutionary relationship to esterases, lysophospholipases, and haloperoxidases. *J Biol Chem.* 1997. 272:27218-27223.

Karlsson M, Reue K, Xia YR, Lusi AJ, Langin D, Tornqvist H, Holm C. Exon-intron organization and chromosomal localization of the mouse monoglyceride lipase gene. *Gene* 2001. 272:11-18.

Kathuria S, Gaetani S, Fegley D, Valino F, Duranti A, Tontini A, Mor M, Tarzia G, La Rana G, Calignano A, Giustino A, Tattoli M, Palmery M, Cuomo V, Pomelli D. Modulation of anxiety through blockade of anandamide hydrolysis. *Nat Med.* 2003. 9:76-81.

Katona I, Urbán GM, Wallace M, Ledent C, Jung KM, Piomelli D, Mackie K, Freund TF. Molecular composition of the endocannabinoid system at glutamatergic synapses. *J Neurosci.* 2006. 26:5628-5637.

Kiernan JA. Dyes and other colorants in microtechnique and biomedical research. *Coloration Technology.* 2006. 122:1-21.

Kim J, Alger BE. Inhibition of cyclooxygenase-2 potentiates retrograde endocannabinoid effects in hippocampus. *Nat Neurosci.* 2004. 7:697-698.

Kobayashi Y, Arai S, Waku K, Sugiura T. Activation by 2-arachidonylethanolamide, an endogenous cannabinoid receptor ligand, of p42/44 mitogen-activated protein kinase in HL-60 cells. *Journal of Biochemistry.* 2001. 129:665-669.

Konrad RJ, Major CD, Wolf BA. Diacylglycerol hydrolysis to arachidonic acid is necessary for insulin secretion from isolated pancreatic islets: sequential actions of diacylglycerol and monoacylglycerol lipases. *Biochemistry*. 1994. 33:13284-13294.

Kozak KR, Crews BC, Morrow JD, Wang LH, Ma YH, Weinander R, Jakobsson PJ, Marnett LJ. Metabolism of the endocannabinoids, 2-arachidonylglycerol and anandamide, into prostaglandin, thromboxane, and prostacyclin glycerol esters and ethanolamides. *J Biol Chem*. 2002. 277:44877-85.

Leung D, Saghatelian A, Simon GM, Cravatt BF. Inactivation of N-acyl phosphatidylethanolamine phospholipase D reveals multiple mechanisms for the biosynthesis of endocannabinoids. *Biochemistry*. 2006. 45:4720–4726.

Lichtman AH, Hawkins EG, Griffin G, Cravatt BF. Pharmacological activity of fatty acid amides is regulated, but not mediated, by fatty acid amide hydrolase in vivo. *J Pharmacol Exp Ther*. 2002. 302:73-79.

Ligresti A, Morera E, Van Der Stelt M, Monory K, Lutz B, Ortar G, Di Marzo V. Further evidence for the existence of a specific process for the membrane transport of anandamide. *Biochem J*. 2004. 380:265–272.

Liu J, Wang L, Harvey-White J, Osei-Hyiaman D, Razdan R, Gong Q, Chan AC, Zhou Z, Huang BX, Kim HY, Kunos G. A biosynthetic pathway for anandamide. *Proc Natl Acad Sci USA*. 2006. 103:13345–13350.

Liu J, Wang L, Harvey-White J, Huang BX, Kim HY, Luquet S, Palmiter RD, Krystal G, Rai R, Mahadevan A, Razdan RK, Kunos G. Multiple pathways involved in the biosynthesis of anandamide. *Neuropharmacology*. 2008. 54:1–7.

López-Rodríguez ML, Viso A, Ortega-Gutiérrez S, Fowler CJ, Tiger G, de Lago E, Fernández-Ruiz J, Ramos JA. Design, synthesis, and biological evaluation of new inhibitors of the endocannabinoid uptake: comparison with effects on fatty acid amidohydrolase. *J Med Chem*. 2003. 46:1512–1522.

Lu Q, Straiker A, Lu Q, Maguire G. Expression of CB2 cannabinoid receptor mRNA in adult rat retina. *Vis Neurosci*. 2000. 17:91-95.

Maccarrone M, van der Stelt M, Rossi A, Veldink GA, Vliegthart JF, Agrò AF. Anandamide hydrolysis by human cells in culture and brain. *J Biol Chem*. 1998. 273:32332–32339.

Maccarrone M, Bari M, Finazzi-Agrò A. A sensitive and specific radiochromatographic assay of fatty acid amide hydrolase activity. *Anal Biochem*. 1999. 267:314–318.

Maccarrone M, Lorenzon T, Bari M, Melino G, Finazzi-Agrò A. Anandamide induces apoptosis in human cells via vanilloid receptors. Evidence for a protective role of cannabinoid receptors. *J Biol Chem*. 2000a. 275:31938-31945.

Maccarrone M, Bari M, Lorenzon T, Bisogno T, Di Marzo V, Finazzi-Agrò A. Anandamide uptake by human endothelial cells and its regulation by nitric oxide. *J Biol Chem*. 2000b. 275:13484–13492.

Maccarrone M, Di Rienzo M, Battista N, Gasperi V, Guerrieri P, Rossi A, Finazzi-Agrò A. The endocannabinoid system in human keratinocytes. Evidence that anandamide inhibits epidermal differentiation through CB1 receptor-dependent inhibition of protein kinase C, activation protein-1, and transglutaminase. *J Biol Chem*. 2003a. 278:33896–33903.

Maccarrone M, Finazzi-Agro A. The endocannabinoid system, anandamide and the regulation of mammalian cell apoptosis. *Cell Death Differ*. 2003b. 10:946-955.

Maccarrone M, Fezza F, Finazzi-Agrò A, Oddi S. Design and synthesis of biotinylated probes for N-acyl-ethanolamines. PCT/EP2006/061988. www.freepatentsonline.com/WO20071_28344.html.

Maccarrone M, Rossi S, Bari M, De Chiara V, Fezza F, Musella A, Gasperi V, Prosperetti C, Bernardi G, Finazzi-Agrò A, Cravatt BF, Centonze D. Anandamide inhibits metabolism and physiological actions of 2-arachidonoylglycerol in the striatum. *Nat Neurosci*. 2008. 11:152-159.

Maier O, Oberle V, Hoekstra D. Fluorescent lipid probes: some properties and applications (a review). *Chem Phys Lipids*. 2002. 116:3-18.

Maione S, Morera E, Marabese I, Ligresti A, Luongo L, Ortar G, Di Marzo V. Antinociceptive effects of tetrazole inhibitors of endocannabinoid inactivation: cannabinoid and non-cannabinoid receptor-mediated mechanisms. *Br J Pharmacol*. 2008. 155:775–782.

Martin S, Parton RG. Lipid droplets: A unified view of a dynamic organelle. *Nat Rev Mol Cell Biol*. 2006. 7:373–378.

Matsuda LA, Lolait SJ, Brownstein MJ, Young AC, Bonner TI. Structure of a cannabinoid receptor and functional expression of the cloned cDNA. *Nature*. 1990. 346:561–564.

McAllister SD, Griffin G, Satin LS, Abood ME. Cannabinoid receptors can activate and inhibit G protein-coupled inwardly rectifying potassium channels in an *Xenopus* oocyte expression system. *J Pharmacol Exp Ther*. 1999. 291:618- 626.

McFarland MJ, Porter AC, Rakhshan FR, Rawat DS, Gibbs RA, Barker EL. A role for caveolae/lipid rafts in the uptake and recycling of the endogenous cannabinoid anandamide. *J. Biol. Chem*. 2004a. 279:41991–41997.

McFarland MJ, Barker EL. Anandamide transport. *Pharmacol Ther*. 2004b. 104:117–135.

McKinney MK, Cravatt BF. Structure and function of fatty acid amide hydrolase. *Annu. Rev. Biochem*. 2005. 74:411–432.

McPartland JM, Matias I, Di Marzo V, Glass M. Evolutionary origins of the endocannabinoid system. *Gene*. 2006. 370:64-74.

Mechoulam R, Ben-Shabat S, Hanus L, Ligumsky M, Kaminski NE, Schatz AR, Gopher A, Almog S, Martind BR, Compton DR, Pertwee RG, Griffin G, Bayewitch M, Bargf J, Vogelf Z. Identification of an endogenous 2-monoglyceride, present in canine gut, that binds to cannabinoid receptors. *Biochem Pharmacol*. 1995. 50:83–90.

Moore SA, Nomikos GG, Dickason-Chesterfield AK, Schober DA, Schaus JM, Ying BP, Xu YC, Phebus L, Simmons RM, Li D, Iyengar S, Felder CC. Identification of a high-affinity binding site involved in the transport of endocannabinoids. *Proc Natl Acad Sci USA*. 2005. 102:17852–17857.

Mor M, Rivara S, Lodola A, Plazzi PV, Tarzia G, Duranti A, Tontini A, Piersanti G, Kathuria S, Piomelli D. Cyclohexylcarbamic acid 3'- or 4'-substituted biphenyl-3-yl esters as fatty acid amide hydrolase inhibitors: Synthesis, quantitative structure-activity relationships, and molecular modeling studies. *J Med Chem*. 2004. 47:4998–5008.

Morishita J, Okamoto Y, Tsuboi K, Ueno M, Sakamoto H, Maekawa N, Ueda N. Regional distribution and age-dependent expression of N-acylphosphatidylethanolamine-hydrolyzing phospholipase D in rat brain. *J Neurochem*. 2005. 94:753–762.

Mulder AM, Cravatt BF. Endocannabinoid metabolism in the absence of fatty acid amide hydrolase (FAAH): discovery of phosphorylcholine derivatives of N-acyl ethanolamines. *Biochemistry*. 2006. 45:11267-11277.
Munro S, Thomas KL, Abu-Shaar M. Molecular characterization of a peripheral receptor for cannabinoids. *Nature*. 1993. 365:61–65.

Munro S, Thomas KL, Abu-Shaar M. Molecular characterization of a peripheral receptor for cannabinoids. *Nature*. 1993. 365:61-65.

Muthian S, Nithipatikom K, Campbell WB, Hillard CJ. Synthesis and characterization of a fluorescent substrate for the N-arachidonylethanolamine (anandamide) transmembrane carrier. *J. Pharmacol Exp Ther*. 2000. 293:289–295.

Nakane S, Oka S, Arai S, Waku K, Ishima Y, Tokumura A, Sugiura T. 2-Arachidonoyl-sn-glycero-3-phosphate, an arachidonic acid-containing lysophosphatidic acid: occurrence and rapid enzymatic conversion to 2-arachidonoyl-sn-glycerol, a cannabinoid receptor ligand, in rat brain. *Arch Biochem Biophys*. 2002. 402:51-58.

Nan X, Potma EO, Xie XS. Nonperturbative chemical imaging of organelle transport in living cells with coherent anti-stokes Raman scattering microscopy. *Biophys J*. 2006. 91:728–735.

Oddi S, Bari M, Battista N, Barsacchi D, Cozzani I, Maccarrone M. Confocal microscopy and biochemical analysis reveal spatial and functional separation between anandamide uptake and hydrolysis in human keratinocytes. *Cell Mol Life Sci.* 2005. 62:386–395.

Okamoto Y, Morishita J, Tsuboi K, Tonai T, Ueda N. Molecular characterization of a phospholipase D generating anandamide and its congeners. *J. Biol. Chem.* 2004. 279:5298–5305.

Ortar G, Ligresti A, De Petrocellis L, Morera E, Di Marzo V. Novel selective and metabolically stable inhibitors of anandamide cellular uptake. *Biochem Pharmacol.* 2003. 65:1473–1481.

Ortega-Gutierrez S, Hawkins EG, Viso A, Lopez-Rodriguez ML, Cravatt BF. Comparison of anandamide transport in FAAH wild-type and knockout neurons: evidence for contributions by both FAAH and the CB1 receptor to anandamide uptake. *Biochemistry.* 2004. 43:8184–8190.

Pasquariello N, Catanzaro G, Marzano V, Amadio D, Barcaroli D, Oddi S, Federici G, Urbani A, Finazzi-Agrò A, Maccarrone M. Characterization of the endocannabinoid system in human neuronal cells and proteomic analysis of anandamide-induced apoptosis. *J Biol Chem.* 2009. 284:29413-29426.

Patel TB, Du Z, Pierre S, Cartin L, Scholich K. Molecular biological approaches to unravel adenylyl cyclase signalling and function. *Gene.* 2001. 269:13–25.

Pertwee RG. Pharmacology of cannabinoid CB1 and CB2 receptors. *Pharmacol Ther.* 1997. 74:129-180.

Pertwee RG. Cannabinoid receptors and pain. *Prog Neurobiol.* 2001. 63:569-611.

Pertwee RG, Ross RA. Cannabinoid receptors and their ligands. *Prostaglandins Leukot Essent Fatty Acids.* 2002. 66:101–121.

Piomelli D, Beltramo M, Glasnapp S, Lin SY, Goutopoulos A, Xie XQ, Makriyannis A. Structural determinants for recognition and translocation by

the anandamide transporter. *Proc. Natl. Acad. Sci. USA.* 1999. 96:5802–5807.

Piomelli D. The molecular logic of endocannabinoid signalling. *Nature Rev Neurosci.* 2003. 4:873-884.

Porter AC, Sauer JM, Knierman MD, Becker GW, Berna MJ, Bao J, Nomikos GG, Carter P, Bymaster FP, Leese AB, Felder CC. Characterization of a novel endocannabinoid, virodhamine, with antagonist activity at the CB1 receptor. *J Pharmacol Exp Ther.* 2002. 301:1020–1024.

Rakhshan F, Day TA, Blakely RD, Barker EL. Carrier-mediated uptake of the endogenous cannabinoid anandamide in RBL-2H3 cells. *J Pharmacol Exp Ther.* 2000. 292:960–967.

Ross RA, Craib SJ, Stevenson LA, Pertwee RG, Henderson A, Toole J, Ellington HC. Pharmacological characterization of the anandamide cyclooxygenase metabolite: prostaglandin E2 ethanolamide. *J Pharmacol Exp Ther.* 2002. 301:900-907.

Ryberg E, Larsson N, Sjögren S, Hjorth S, Hermansson NO, Leonova J, Elebring T, Nilsson K, Drmota T, Greasley PJ. The orphan receptor GPR55 is a novel cannabinoid receptor. *Br J Pharmacol.* 2007.152:1092-1101.

Sang N, Zhang J, Chen C. PGE2 glycerol ester, a COX-2 oxidative metabolite of 2-arachidonoyl glycerol, modulates inhibitory synaptic transmission in mouse hippocampal neurons. *J Physiol.* 2006. 572:735-745.

Sawzdargo M, Nguyen T, Lee DK, Lynch KR, Cheng R, Heng HH., George SR, O'Dowd BF. Identification and cloning of three novel human G protein-coupled receptor genes GPR52, PsiGPR53 and GPR55: GPR55 is extensively expressed in human brain. *Brain Res Mol Brain Res.* 1999. 64:193-198.

Schatz AR, Lee M, Condie RB, Pulaski JT, Kaminski NE. Cannabinoid receptors CB1 and CB2: a characterization of expression and adenylate cyclase modulation within the immune system. *Toxicological Applications in Pharmacology.*1997.142:278–287.

Siemens J, Zhou S, Piskorowski R, Nikai T, Lumpkin EA, Basbaum AI, King D, Julius D. Spider toxins activate the capsaicin receptor to produce inflammatory pain. *Nature*. 2006. 444:208-212.

Simon GM, Cravatt BF. Endocannabinoid biosynthesis proceeding through glycerophospho-N-acyl ethanolamine and a role for alpha/beta-hydrolase 4 in this pathway. *J Biol Chem*. 2006. 281:26465–26472.

Simpson CM, Itabe H, Reynolds CN, King WC, Glomset JA. Swiss 3T3 cells preferentially incorporate sn-2-arachidonoyl monoacylglycerol into sn-1-stearoyl-2-arachidonoyl phosphatidylinositol. *J Biol Chem*. 1991. 266:15902-15909.

Slanina KA, Roberto M, Schweitzer P. Endocannabinoids restrict hippocampal long-term potentiation via CB1. *Neuropharmacology*. 2005. 49:660-668.

Starowicz K, Nigam S, Di Marzo V. Biochemistry and pharmacology of endovanilloids. *Pharmacol Ther*. 2007. 114:13-33.

Stella N, Schweitzer P, and Piomelli D. A second endogenous cannabinoid that modulates long-term potentiation. *Nature*. 1997. 388:773-778.

Stella, N.; Piomelli, D. Receptor-dependent formation of endogenous cannabinoids in cortical neurons. *Eur. J. Pharmacol.*, 2001. 425:189.

Sugiura T, Kondo S, Sukagawa A, Nakane S, Shinoda A, Itoh K, Yamashita A, Waku K. 2-Arachidonoylglycerol: a possible endogenous cannabinoid receptor ligand in brain. *Biochem Biophys Res Commun*. 1995. 215:89–97.

Sugiura T, Kodaka T, Kondo S, Tonegawa T, Nakane S, Kishimoto S, Yamashita A, Waku K. 2-Arachidonoylglycerol, a putative endogenous cannabinoid receptor ligand, induces rapid, transient elevation of intracellular free Ca²⁺ in neuroblastoma x glioma hybrid NG108-15 cells. *Biochem Biophys Res Commun*. 1996. 229:58-64.

Sugiura T, Yoshinaga N, Kondo S, Waku K, Ishima Y. Generation of 2-arachidonoylglycerol, an endogenous cannabinoid receptor ligand, in

microtoxinin-administered rat brain. *Biochem Biophys Res Commun.* 2000. 271:654-658.

Sun YX, Tsuboi K, Okamoto Y, Tonai T, Murakami M, Kudo I, Ueda N. Biosynthesis of anandamide and N-palmitoylethanolamine by sequential actions of phospholipase A2 and lysophospholipase D. *Biochem J.* 2004. 380:749-756.

Szallasi A, Szabo T, Biro T, Modarres S, Blumberg PM, Krause JE, Cortright DN, Appendino G. Resiniferatoxin-type phorboid vanilloids display capsaicin-like selectivity at native vanilloid receptors on rat DRG neurons and at the cloned vanilloid receptor VR1. *Br J Pharmacol.* 1999. 128:428-434.

Terai T, Nagano T. Fluorescent probes for bioimaging applications. *Curr Opin Chem Biol.* 2008. 12:515-521.

Tsou K, Nogueron MI, Muthian S, Sañudo-Pena MC, Hillard CJ, Deutsch DG, Walker JM. Fatty acid amide hydrolase is located preferentially in large neurons in the rat central nervous system as revealed by immunohistochemistry. *Neurosci Lett.* 1998. 254:137-140.

Tsuboi K, Sun YX, Okamoto Y, Araki N, Tonai T, Ueda N. Molecular characterization of N-acyl ethanolamine-hydrolyzing acid amidase, a novel member of the cholesterylglycine hydrolase family with structural and functional similarity to acid ceramidase. *J Biol Chem.* 2005. 280:11082-11092.

Tsutsumi T, Kobayashi T, Ueda H, Yamauchi E, Watanabe S, Okuyama H. Lysophosphoinositide-specific phospholipase C in rat brain synaptic plasma membranes. *Neurochem Res.* 1994. 19:399-406.

Ueda H, Kobayashi T, Kishimoto M, Tsutsumi T, Okuyama H. A possible pathway of phosphoinositide metabolism through EDTA-insensitive phospholipase A1 followed by lysophosphoinositide-specific phospholipase C in rat brain. *J Neurochem.* 1993a. 61:1874-1881.

Ueda H, Kobayashi T, Kishimoto M, Tsutsumi T, Watanabe S, Okuyama H. The presence of Ca²⁺-independent phospholipase A1 highly specific for

phosphatidylinositol in bovine brain. *Biochem Biophys Res Commun.* 1993b. 195:1272-1279.

Ueda N, Kurahashi Y, Yamamoto S, Tokunaga T. Partial purification and characterization of the porcine brain enzyme hydrolyzing and synthesizing anandamide. *J Biol Chem.* 1995a. 270:23823–23827.

Ueda N, Yamamoto K, Yamamoto S, Tokunaga T, Shirakawa E, Shinkai H, Ogawa M, Sato T, Kudo I, Inoue K. Lipoxygenase-catalyzed oxygenation of arachidonylethanolamide, a cannabinoid receptor agonist. *Biochim Biophys Acta.* 1995b. 1254:127-1234.

Ueda N, Yamanaka K, Yamamoto S. Purification and characterization of an acid amidase selective for N-palmitoylethanolamine, a putative endogenous anti-inflammatory substance. *J Biol Chem.* 2001. 276:35552-35557.

van der Stelt M, Di Marzo V. Endovanilloids. Putative endogenous ligands of transient receptor potential vanilloid 1 channels. *Eur J Biochem.* 2004. 271:1827-1834.

van der Stelt M, Di Marzo V. Endovanilloids. Putative endogenous ligands of transient receptor potential vanilloid 1 channels. *Eur J Biochem.* 2004. 271:1827–1834.

Wei BQ, Mikkelsen TS, McKinney MK, Lander ES, Cravatt BF. A second fatty acid amide hydrolase with variable distribution among placental mammals. *J Biol Chem.* 2006. 281:36569-36578.

Williams EJ, Walsh FS, Doherty P. The FGF receptor uses the endocannabinoid signaling system to couple to an axonal growth response. *J Cell Biol.* 2003. 160:481-486.

Witting A, Walter L, Wacker J, Moller T, Stella N. P2X7 receptors control 2-arachidonoylglycerol production by microglial cells. *Proc Natl Acad Sci USA.* 2004. 101:3214-3119.

Wolins NE, Rubin B, Brasaemle DL. TIP47 associates with lipid droplets. *J Biol Chem.* 2001. 276:5101–5108.

Yamaji K, Sarker KP, Kawahara K, Iino S, Yamakuchi M, Abeyama K, Hashiguchi T, Maruyama I. Anandamide induces apoptosis in human endothelial cells: its regulation system and clinical implications. *Thromb Haemost.* 2003. 89:875-884.

Yu W, Cassara J, Weller PF. Phosphatidylinositide 3-kinase localizes to cytoplasmic lipid bodies in human polymorphonuclear leukocytes and other myeloid-derived cells. *Blood.*2000. 95:1078–1085.

Zygmunt PM, Petersson J, Andersson DA, Chuang HH, Sorgård M, Di Marzo V, Julius D, Högestätt ED. Vanilloid receptors on sensory nerves mediate the vasodilator action of anandamide. *Nature.* 1999. 400:452-457.

SHORT CURRICULUM VITAE

Dati personali :

- Cognome e nome: Chiara De Simone
- Luogo e data di nascita: Latina, 23/03/1979
- Residenza: Latina, via Boccioni, 5, 04100
- Codice fiscale: DSMCHR79C63E472S
- Telefono: 3388733346
- Mail: chiaradesimone79@gmail.com

Titoli di Studio :

- Diploma scientifico, conseguito nel luglio del 1998 presso il liceo scientifico G.B. Grassi di Latina con la votazione di 60/60.
- Laurea in Chimica (ordinamento quinquennale), conseguita il 26/05/2005 presso l'Università degli studi di Roma "La Sapienza" con la votazione di 110/110 e lode; titolo della tesi sperimentale: "Meccanismo d'azione del farmaco antivirale Ribavirina", svolta presso l'istituto di Cristallografia del CNR di Roma (Montelibretti), sotto la guida del Dott. Luciano Cellai.

Esperienze lavorative :

- Vincitrice nel luglio 2005 dell'assegno di ricerca CNR nell'ambito del programma di ricerca Sintesi di modelli di acidi nucleici, da svolgere presso l'istituto di Cristallografia del CNR di Roma sotto la direzione del Dott. Luciano Cellai.
- Titolare dal 15/12/05 al 15/04/06 del contratto di collaborazione scientifica "Studio del sistema endocannabinoide nell'invasività tumorale", presso l'Università di Teramo sotto la direzione del Prof. Mauro Maccarrone.
- Titolare dal 1/06/06 al 30/09/06 del contratto di collaborazione scientifica "Sintesi ed analisi di nuovi derivati dell'Anandamide", presso l'Università di Teramo sotto la direzione del Prof. Mauro Maccarrone.
- Titolare da ottobre 2006 sino a Dicembre 2009 della borsa di dottorato in Biochimica e Biologia Molecolare, facoltà di Medicina e Chirurgia, presso l'Università degli studi di Roma "Tor Vergata" sotto la direzione del Prof. Alessandro Finazzi-Agrò e del Prof. Mauro Maccarrone.

LIST OF PUBLICATIONS

- Gattinoni S*, **De Simone C***, Dalla valle S, Fezza F, Nannei R, Amadio D, Minetti P, Quattrociochi G, Caprioli A, Borsini F, Cabri W, Penco S, Merlini L, Maccarrone M. Enol carbamates as inhibitors of fatty acid amide hydrolase (FAAH) endowed with high selectivity towards the other elements of the endocannabinoid system. (*These authors contributed equally to the study) *submitted*
- Oddi S, Fezza F, Pasquariello N, D'Agostino A, Catanzaro G, **De Simone C**, Rapino C, Finazzi-Agrò A, Maccarrone M. Molecular identification of albumin and Hsp70 as cytosolic anandamide-binding proteins. *Chem Biol.* 2009. 16:624-632.
- Fezza F, **De Simone C**, Amadio D, Maccarrone M. Fatty acid amide hydrolase: a gate-keeper of the endocannabinoid system. *Subcell Biochem.* 2008; 49:101-132.
- Fezza F, Oddi S, Di Tommaso M, **De Simone C**, Rapino C, Pasquariello N, Dainese E, Finazzi-Agrò A, Maccarrone M. Characterization of biotin-anandamide, a novel tool for the visualization of anandamide accumulation, *J Lipid Res.* 2008. 49:1216-1223.
- Oddi S, Fezza F, Pasquariello N, **De Simone C**, Rapino C, Dainese E, Finazzi-Agrò A, Maccarrone M. Evidence for the intracellular accumulation of anandamide in adiposomes. *Cell Mol Life Sci.* 2008. 65:840-850.
- Bari M, Oddi S, **De Simone C**, Spagnolo P, Gasperi V, Battista N, Centonze D, Maccarrone M. Type-1 cannabinoid receptors colocalize with caveolin-1 in neuronal cells. *Neuropharmacology.* 2008. 54:45-50.
- Nucci C, Gasperi V, Tartaglione R, Cerulli A, Terrinoni A, Bari M, **De Simone C**, Agrò AF, Morrone LA, Corasaniti MT, Bagetta G, Maccarrone M. Involvement of the endocannabinoid system in retinal damage after high intraocular pressure-induced ischemia in rats. *Invest Ophthalmol Vis Sci.* 2007. 48:2997-3004.

COPY OF RELAVANT PUBLICATIONS

COPY OF RELAVANT PUBLICATIONS

- Oddi S, Fezza F, Pasquariello N, D'Agostino A, Catanzaro G, **De Simone C**, Rapino C, Finazzi-Agrò A, Maccarrone M. Molecular identification of albumin and Hsp70 as cytosolic anandamide-binding proteins. *Chem Biol.* 2009. 16:624-632.
- Fezza F, Oddi S, Di Tommaso M, **De Simone C**, Rapino C, Pasquariello N, Dainese E, Finazzi-Agrò A, Maccarrone M. Characterization of biotin-anandamide, a novel tool for the visualization of anandamide accumulation, *J Lipid Res.* 2008. 49:1216-1223.

ACKNOWLEDGMENTS

I wish to express my gratitude to Prof. Alessandro Finazzi-Agrò, to my Prof. Mauro Maccarrone, to Dott.ssa Filomena Fezza and to all my colleagues.